



Michigan Technological University  
*Create the Future* Digital Commons @ Michigan Tech

---

Dissertations, Master's Theses and Master's  
Reports - Open

Dissertations, Master's Theses and Master's  
Reports

---

2011

## Structure and properties of graphene nano disks (GND) with and without edge-dopants

Pubodee Ratana-arsanarom  
*Michigan Technological University*

Follow this and additional works at: <https://digitalcommons.mtu.edu/etds>

 Part of the [Engineering Science and Materials Commons](#)


Copyright 2011 Pubodee Ratana-arsanarom

---

### Recommended Citation

Ratana-arsanarom, Pubodee, "Structure and properties of graphene nano disks (GND) with and without edge-dopants", Master's Thesis, Michigan Technological University, 2011.  
<https://doi.org/10.37099/mtu.dc.etds/29>

Follow this and additional works at: <https://digitalcommons.mtu.edu/etds>

 Part of the [Engineering Science and Materials Commons](#)

STRUCTURE AND PROPERTIES OF GRAPHENE NANO DISKS (GND) WITH  
AND WITHOUT EDGE-DOPANTS

By

Pubodee Ratana-arsanarom

A THESIS

Submitted in partial fulfillment of the requirements for the degree of

MASTER OF SCIENCE

(Materials Science and Engineering)

MICHIGAN TECHNOLOGICAL UNIVERSITY

2011

© 2011 Pubodee Ratana-arsanarom

This thesis, “Structures and Properties of Graphene Nano Disks (GND) with and Without Edge-dopants,” is hereby approved in partial fulfillment of the requirements for the degree of MASTER OF SCIENCE IN THE FIELD OF MATERIALS SCIENCE AND ENGINEERING.

Department of Materials Sciences and Engineering

Signatures:

Thesis Advisor: \_\_\_\_\_  
Yun Hang Hu

Department Chair: \_\_\_\_\_  
Mark Plichta

Date: \_\_\_\_\_

## TABLE OF CONTENTS

<b>List of Figures</b> .....	5
<b>List of Tables</b> .....	7
<b>Acknowledgements</b> .....	8
<b>Abstract</b> .....	9
<b>Chapter 1     Introduction and Background</b> .....	11
1.1     Synthesis of graphene .....	11
1.2     Properties of graphene .....	13
1.3     Doped graphene .....	14
<b>Chapter 2     Calculation Methods</b> .....	18
2.1     Ab initio methods for molecules and materials .....	18
2.2     Density Functional Theory (DFT) .....	19
2.3     Selection for calculation methods in this research.....	21
<b>Chapter 3     Structures and Properties of Graphene Nano Disks (GND)</b> .....	23
3.1     Structures of graphene nano disks .....	22
3.2     Stability of graphene nano disks .....	31
3.3     HOMO-LUMO energy gap of graphene nano disk .....	32



<b>Chapter 4</b>	<b>Structure and Properties of Graphene Nano Disk (GND)</b>	
	<b>with Edge-doping</b> .....	34
4.1	Structures of graphene nano disks with edge-dopants .....	34
4.2	Stability of graphene nano disks with edge-dopants.....	64
4.3	HOMO-LUMO energy gap of graphene nano disk with edge-dopants .....	65
<b>Chapter 5</b>	<b>Conclusion</b> .....	67
<b>References</b> .....		69

## List of Figures

Figure 3.1	Structure of $C_6$ graphene nano disk .....	23
Figure 3.2	Structure of $C_{24}$ graphene nano disk .....	24
Figure 3.3	Structure of $C_{54}$ graphene nano disk .....	26
Figure 3.4	Structure of $C_{96}$ graphene nano disk .....	28
Figure 3.5	Stabilization energy ( $E_{st}$ ) of graphene vs. it number of carbon atoms .....	31
Figure 3.6	HOMO-LUMO energy gap of graphene nano disks.....	33
Figure 4.1	Structure of $C_6$ graphene nano disk with H-dopants.....	35
Figure 4.2	Structure of $C_{24}$ graphene nano disk with H-dopants .....	36
Figure 4.3	Structure of $C_{54}$ graphene nano disk with H-dopants .....	37
Figure 4.4	Structure of $C_{96}$ graphene nano disk with H-dopants .....	39
Figure 4.5	Structure of $C_6$ graphene nano disk with F-dopants .....	42
Figure 4.6	Structure of $C_{24}$ graphene nano disk with F-dopants .....	43
Figure 4.7	Structure of $C_{96}$ graphene nano disk with F-dopants .....	44
Figure 4.8	Structure of $C_6$ graphene nano disk with OH-dopants.....	47
Figure 4.9	Structure of $C_{24}$ graphene nano disk with OH-dopants .....	48
Figure 4.10	Structure of $C_{54}$ graphene nano disk with OH-dopants .....	50
Figure 4.11	Structure of $C_{96}$ graphene nano disk with OH-dopants .....	54
Figure 4.12	Structure of $C_6$ graphene nano disk with Li-dopants .....	60
Figure 4.13	Structure of $C_{24}$ graphene nano disk with Li-dopants.....	61
Figure 4.14	Structure of $C_{54}$ graphene nano disk with Li-dopants.....	62

Figure 4.15	Stabilization energy ( $E_{st}$ ) of graphene vs. it number of carbon atoms: (a) without edge doping, (b) H-doped, (c) Li-doped, (d) F-doped, and (e) OH-doped .....	64
Figure 4.16	HOMO-LUMO energy gap of graphene nano disks; (a) without doping, (b) H-doped, (c) Li-doped, (d) F-doped, and (e) OH-doped.....	66

## **List of Tables**

Table 1	Summary of graphene properties .....	14
---------	--------------------------------------	----

## **ACKNOWLEDGEMENTS**

There are many people that I would like to thank for their help over the course of my studies at Michigan Tech. Specially; I would like to thank my advisor, Dr. Yun Hang Hu, for all of his direction and support over the past years. Without his expertise in the area of the computational chemistry, the completion of this work would not have been possible.

## ABSTRACT

Graphene is one of the most important materials. In this research, the structures and properties of graphene nano disks (GND) with a concentric shape were investigated by Density Functional Theory (DFT) calculations, in which the most effective DFT methods - B3lyp and Pw91pw91 were employed.

It was found that there are two types of edges - Zigzag and Armchair in concentric graphene nano disks (GND). The bond length between armchair-edge carbons is much shorter than that between zigzag-edge carbons. For C24 GND that consists of 24 carbon atoms, only armchair edge with 12 atoms is formed. For a GND larger than the C24 GND, both armchair and zigzag edges co-exist. Furthermore, when the number of carbon atoms in armchair-edge are always 12, the number of zigzag-edge atoms increases with increasing the size of a GND. In addition, the stability of a GND is enhanced with increasing its size, because the ratio of edge-atoms to non-edge-atoms decreases.

The size effect of a graphene nano disk on its HOMO-LUMO energy gap was evaluated. C6 and C24 GNDs possess HOMO-LUMO gaps of 1.7 and 2.1eV, respectively, indicating that they are semi-conductors. In contrast, C54 and C96 GNDs are organic metals, because their HOMO-LUMO gaps are as low as 0.3 eV.

The effect of doping foreign atoms to the edges of GNDs on their structures, stabilities, and HOMO-LUMO energy gaps were also examined. When foreign atoms are attached to the edge of a GND, the original unsaturated carbon atoms become saturated. As a result, both of the C-C bonds lengths and the stability of a GND increase.

Furthermore, the doping effect on the HOMO-LUMO energy gap is dependent on the type of doped atoms. The doping H, F, or OH into the edge of a GND increases its HOMO-LUMO energy gap. In contrast, a Li-doped GND has a lower HOMO-LUMO energy gap than that without doping. Therefore, Li-doping can increase the electrical conductance of a GND, whereas H, F, or OH-doping decreases its conductance.

## Chapter 1

### Introduction and Background

Dimensions are the most characteristic to define the properties of materials. The bonding flexibility of carbon created various structures of carbon materials. Graphite and diamond are well-known three-dimensional carbon allotropes. Furthermore, the zero-dimensional carbon “fullerenes” and one-dimensional carbon “nanotubes” were also discovered in 1985 (1) and 1990 (2), respectively. However, two-dimensional carbon “graphene”, which is a single atom thickness layer of graphite, has been ignored for a long time. Graphene was originally described in terms of the combination of graphite and the suffix -ene by Hanns-Peter Boehm (3), who used this term to describe the single layer of carbon. However, following the argument between Landau and Peierls, the two dimension of carbon allotrope that strictly 2D crystals is thermodynamically unstable and could not exist (4,5). In 1994, Shioyama has successfully extracted graphene from graphite by graphite intercalation compounds. However, in this case, the graphene is not in the single sheet state (6). In 2004, this situation was completely changed with the demonstration of the new technique for exfoliated a single graphene (7). This pioneering work has stimulated worldwide attempts to explore properties and applications of graphene. As a result, graphene has become the most promising two-dimensional material (8-20).

#### *1.1 Synthesis of graphene*

In 2004, a research group at Manchester University obtained a graphene by the mechanical exfoliation of graphite, namely, graphite crystals were repeatedly split by



cohesive tape to decreasingly the thickness of graphite layers (7). The tape, which was attached with the residues of the optically transparent flakes, was dissolved in acetone, followed by reduction of the flakes into the monolayers and deposited on a silicon wafer. Afterward, this group used a new procedure to simplify the previous technique by using dry deposition. The graphene obtained from this new approach is a relatively large crystallites size.

Epitaxial growth on SiC substrate is achieved by heating a silicon carbide (SiC) to a high temperature ( $>1100\text{ }^{\circ}\text{C}$ ) (21). The properties of obtained graphene, such as thickness, mobility and carrier density, are dependent upon the heating temperature, time and the dimension of SiC substrate.

Graphene can also be synthesis via chemical vapor deposition (CVD) technique, namely, graphene can be grown on metal surfaces by catalytic decomposition of hydrocarbons or carbon oxide (22-24). When hydrocarbon (or carbon oxide) contact a heated surface, it can decompose into carbon atoms and hydrogen gas (or oxygen gas) on the surface, and the carbon atoms will form a graphene single-layer.

As a promising route for graphene synthesis, the oxidation of graphite followed by reduction has been widely employed to produce a large amount of graphene (25-28). In this approach, graphite can be oxidized via its reaction with  $\text{KClO}_3$  (potassium chloride) and  $\text{HNO}_3$  (nitric acid) (27) or with  $\text{KMnO}_4$  (potassium permanganate) and concentrated  $\text{H}_2\text{SO}_4$  (sulfuric acid) (28). Currently, many thermal and mechanical approaches are available for the exfoliation of graphite oxide into graphene oxide single-layer, but ultrasonic treatment is commonly used. Finally, the reduction of graphene

oxide single-layers into graphene sheets can be achieved by thermal or chemical treatments (25).

## ***1.2 Properties of graphene***

The single sheet of graphene exhibits many unique properties (29-33), which were summarized in Table 1. For example, graphene has been recognized a unique mixture of a semiconductor and a metal with extraordinary electronic excitations, which can be described in terms of Dirac fermions that travel in a curved space (31). In contrast to the case of regular metals and semi-conductors, the electrons in graphene are nearly insensitive to disorder and electron-electron interactions.

**Table 1.** Summary of graphene properties (29)

Properties	Value	Observations
Length of the lattice	$a = \sqrt{3}a_{C-C}$	$a_{C-C} \approx 1.42 \text{ \AA}$ is the
Vector		carbon bond length (31)
Surface area	2600m <sup>2</sup> /g	Theoretical prediction (66)
Mobility	15,000 cm <sup>2</sup> V <sup>-1</sup> s <sup>-1</sup> (typical) 200,000 cm <sup>2</sup> V <sup>-1</sup> s <sup>-1</sup> (Intrinsic)	At room temperature (13,67)
Means free path (ballistic transport)	300-500 nm	At room temperature (68)
Fermi velocity	$c/300=1,000,000 \text{ m/s}$	At room temperature (68)
Electron effective mass	$0.06 m_o$	At room temperature (68)
Hole effective mass	$0.03 m_o$	At room temperature (68)
Thermal conductivity	$(5.3 \pm 0.48) \times 10^3 \text{ W/mK}$	Better thermal conductivity than in most crystals (69)
Breaking strength	40N/m	Reaching theoretical limit (70)
Young modulus	1.0 TPa	Ten times greater than in steel (70)
Opacity	2.3%	Visible light (71)
Optical transparency	97.7%	Visible light (71)

### **1.3 Doped graphene**

Graphene is a suitable material for electronic industrial and chemical processes. However, only graphene itself is not sufficiently for electronic devices and catalysts due to the lack of controlling the chirality of carbon atoms in its structure to modify the electronic properties. The doping foreign atoms into graphene are attracting more attention to manipulate the electronic and chemical properties.

Chen and his coworkers evaluated the catalytic oxidation of CO on Fe-embedded graphene by means of first-principles computations (34). The reactions between the adsorbed O<sub>2</sub> with CO via both Langmuir-Hinshelwood (LH) and Eley-Rideal (ER) mechanisms were examined, which indicated that the Fe embedded graphene exhibited good catalytic activity for the CO oxidation via the ER mechanism. Åhlgren et al. employed classical molecular dynamics simulations combined with density functional theory to evaluate the feasibility of low-energy ion irradiation for doping B/N into graphene (35). Their results showed that 50 eV can be used as an optimized irradiation energy, with which substitution probabilities for B and N elements are 40 and 55%, respectively. Furthermore, they concluded that the ion irradiation is an effective approach to create C-B/N hybrid structures for nanoelectronics. Ao et al. theoretically examined the effect of doping Al on hydrogen storage in graphene (36), indicating that C and H<sub>2</sub> electronic structures could be altered by doped Al.

The edges of graphene play an important role in its structures and properties. Nakada and Mitsutaka found that the edge state possesses the charge density localized at the sites of zigzag edge (37). Zhao et al. employed a semi-model to evaluate the relaxation effects of edge bonds for GNRFETs (graphene nanoribbon field-effect transistors) with AGNR (armchair-edge graphene) (38). They showed that the edges of AGNRs remarkably affect quantum capacitance. Furthermore, Sako et al. investigated edge configuration and quantum confinement effects on electron transport in armchair-edged graphene nanoribbons (A-GNRs) with a computational approach. They found that the edge bond relaxation has a significant influence not only on the bandgap energy, but also on the electron effective mass (39). In addition, Oeiras et al. investigated the

electronic and transport properties of defect carbon nanoribbons with ab initio calculations. Their simulations showed that the defect in ribbon edge decreases the energy of the ribbon (40).

The functionalization of graphene edge is demonstrated as a promising approach to modify the properties of graphene. Cervantes-Sodi et al showed that, if armchair ribbons are functionalized at their edge, some electronic states can be created, but their band gap is not significantly affected (41). Ouyang et al. used the density-functional theory (DFT) simulation and a top-of-the-barrier ballistic transport model to reveal the effect of edge-termination on the properties of graphene nanoribbon (GNR), such as channel conductance, quantum capacitance, and carrier injection velocity (42). Furthermore, the H termination was identified to have the largest on current and carrier injection velocity. Berashevich and Chakraborty evaluated the oxidized zigzag edge of graphene (43). They found that the clusters of  $H_2O$  and  $NH_3$  could be formed at the oxidized zigzag edges of graphene, because they can interact with electronegative oxygen. There is a charge transfer from graphene to the adsorbates, and the efficiency of charge donation from graphene is dependent on the location of adsorbates at graphene and its distance from graphene. Cocchi et al theoretically investigated the effect of covalent edge functionalization (with organic functional groups) on the properties of graphene nanostructures and nanojunctions (44). Their analysis shows that functionalization can be designed to tune electron affinities and ionization potentials of graphene flakes, and to control the energy alignment of frontier orbitals in nanometer-wide graphene junctions. The stability of the proposed mechanism was discussed with respect to the functional groups, their number as well as the width of graphene

nanostructures. Their results indicate that different level alignments can be obtained and engineered in order to realize stable all-graphene nanodevices.

From the above, one can see that the properties of graphene can be tuned by doping some elements or functional groups. Furthermore, the edge with and without dopants strongly affects the structure and properties of graphene. However, so far, the edge and doping effects of graphene have been evaluated mainly for graphene ribbons. In this research, we evaluate the effect of edges and dopants on structure and properties of graphene nano disks via density functional theory calculations.

## Chapter 2

### Calculation Methods

#### *2.1 Ab initio methods for molecules and materials*

Ab initio methods are widely used for molecules, clusters, and even large systems via solving the many-body Schrödinger equation (45). Furthermore, the Born-Oppenheimer approximation can allow us to separate the electronic freedom-degrees from the nuclei. As a result, we can consider only electronic variable at a given nuclear configuration. The electronic Schrödinger can be expressed as

$$\hat{H}\Psi = E\Psi \tag{1}$$

Where  $\psi$ ,  $E$ , and  $\hat{H}$  are a wavefunction, the total energy, and the electronic Hamilton, respectively. However, because the Schrödinger equation is too complicated, the largest system, for which the exact eigenfunctions and eigenvalues can be derived from the equation, is the hydrogen molecular ion,  $H_2^+$ . For this reason, the two methods of approximation are most widely used for molecules and materials calculations: the variation principle and perturbation theory.

The exact Hamiltonian operator can be employed for the description of electron motion and the Coulomb interactions of the electron with other charged particles in a system. However, because the exact many-electron wavefunction is unknown, some suitable approximations must be employed. The well-known Hartree-Fock theory established a simple approximation for the many-electron wavefunction—the product of

one-electron wavefunctions, in which each individual electron possesses a one-electron wavefunction (46). Although the Hartree-Fock theory is still applied, its critical drawback is the neglecting of electron correlations, which could lead to a large error. Numerous approaches have been employed to solve this issue. For example, Møller-Plesset perturbation theory considers the correlation as a perturbation of Fock operator. However, calculations based on Møller-Plesset perturbation theory are very expensive, which can be employed only for relative small systems.

In contrast to the Hartree-Fock technique, density functional theory (DFT), which considers the entire electronic system, includes both exchange and correlations at affordable calculation cost. Therefore, DFT has become the most powerful method for relatively large systems.

## ***2.2 Density Functional Theory (DFT)***

In the 1960s, Hohenberg and Kohn demonstrated that the ground state density  $\rho(r)$  of electrons is sufficient in principle to determine not only the energy in the Hartree-Fock approximation, but also the exact many-body energy including all effects beyond Hartree-Fock theory (i.e. correlation) (47), namely, the ground state energy of a system can be correlated with the electron density as follows

$$E[\rho(r)] = F[\rho(r)] + \int [\rho(r)] V_{ext}(r) d^3r \quad (2)$$



The density  $\rho(r)$  minimizing the energy of the system corresponds to the ground state density. This density function is much simpler than wavefunction  $\Psi(r)$ . This Hohenberg-Kohn (HK) theorem provides a novel approach to express many-body system by the density rather than the wavefunctions.

To formulate an effective density  $\rho(r)$ , Kohn and Sham used orthonormal noninteracting single-particle wavefunctions,  $\Psi_i(r)$  as follows (48)

$$\rho(r) = \sum_i |\Psi_i(r)|^2 \quad (3)$$

Thus,  $F[\rho(r)]$  as

$$F[\rho(r)] = \sum_i \frac{\hbar^2}{2m_e} \int \psi_i^* \nabla^2 \psi_i d^3r + \frac{e^2}{2} \int \frac{\rho(r)\rho(r')}{|r-r'|} d^3r d^3r' + E_{xc}[\rho(r)] \quad (4)$$

Where  $E_{xc}[\rho(r)]$  is the exchange-correlation energy. Because the true form of  $E_{xc}$  is unknown, approximation to  $E_{xc}$  is needed. Kohn and sham originally established the local density approximation (LDA) as follows

$$E_{xc}[\rho(r)] = \int \varepsilon_{xc}[\rho(r)] \rho(r) d^3r \quad (5)$$

Where  $\varepsilon_{xc}$  is the exchange-correlation energy per unit volume of a homogeneous electron gas with a density of  $\rho(r)$ . However, LDA tended to a high level of overbinding for molecular systems. To solve this issue, “generalized gradient approximations” (GGA) of the electron density was introduced (49,50). Although the introduction of the density gradient has no significant effect on local properties (such as bond lengths), however it is

can improve the accuracy for energy calculations of a molecule or a relatively large system.

### ***2.3 Selection for calculation methods in this research***

Nano-structure systems challenge molecular-orbital based quantum calculations due to their large sizes. It is well-known that computational time increases sharply with increasing system size, which can prohibit us to exploit the most sophisticated ab initio methods to nano-structured system (51,52). However, electron correlations are taken into account at low computational cost in DFT techniques. Therefore, DFT can be used for nano-clusters with an acceptable accuracy.

It is important to determine the appropriate method for our calculations of relatively large graphene-based systems. The B3lyp is a hybrid DFT, which is the combination between HF and a DFT based on Becke's exchange coupled with the LYP correlation potential (53). The B3lyp, run with a 6-31G(d) or better basis set, is generally the best choice of a model chemistry for most systems. Nevertheless, when the bond lengths of C<sub>60</sub> predicted by B3lyp/6-31G(d) DFT calculations are consistent with experimental data (54-56), the B3lyp calculations overestimated the energy gap of C<sub>60</sub> between the highest occupied molecular orbital (HOMO) and the lowest unoccupied molecular orbital (LUMO) (57). In contrast, our PW91PW91/6-31G(d) DFT calculation for C<sub>60</sub> predicted a HOMO-LUMO energy gap of 1.7113eV, which is in excellent agreement with experimental energy gap (1.7eV) (58). For this reason, B3lyp hybrid DFT with 6-31G(d) basis set was exploited for geometric optimizations of nano graphene disks in this work. Furthermore, energy calculations were carried out by using PW91PW91/6-

31G(d) method with the B3lyp/6-31G(d) optimized geometries. All calculations for geometric optimizations and energies for both straight and bent chains were performed with the Gaussian 03 program (59).

## Chapter 3

### Structures and Properties of Graphene Nano Disks (GND)

Density functional theory (B3lyp and Pw91pw91) calculations were employed to evaluate the structures and properties for graphene nano disks, including (1) the optimization of structures, (2) stability, and (3) HOMO-LUMO energy gaps.

#### *3.1 Structures of graphene nano disks*

First, we optimized geometry of the smallest graphene nano disk (named as C<sub>6</sub> GND) consisting of only 6 carbon atoms as a 6-member ring (Figure 3.1). From Figure 3.1, one can see that the bond-length and angle are 1.3096Å and 120°, respectively. Therefore, this smallest GND has a similar structure as benzene. However, the bond length (1.3906Å) of the GND is smaller than that (1.40Å) of benzene because all carbon atoms in the smallest NGD are unsaturated.

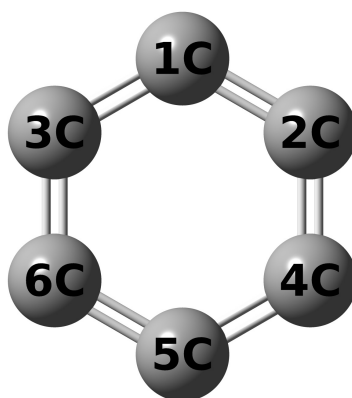


**Figure 3.1 Structure of C<sub>6</sub> graphene nano disk**

Bond length (angstrom)		Atom internal angle (degree)	
1-2:	1.309592	1:	120.00000
2-4:	1.309592	2:	119.99999
4-5:	1.309592	4:	119.99997
5-6:	1.309592	5:	120.00000
6-3:	1.309592	6:	119.99997
3-1:	1.309592	3:	119.99997

When six 6-member rings are formed around the smallest GND, the second graphene disk (named as C<sub>24</sub> GND) with a concentric shape, which contains 24 carbon atoms, is generated (Figure 3.2). The structure of this GND has separated into 4 types of member rings with armchair edge. For the central member ring, bond lengths increases from 1.3096Å to 1.4476Å when compared with C<sub>6</sub> GND. In contrast, the bond angle of the central 6-member ring, which remains unchanged, is still 120°C due to its symmetrical structure. The increase of bond lengths is due to the saturation of the carbon atoms in the C<sub>24</sub> center ring (Figure 3.2). For 2<sup>nd</sup>, 3<sup>rd</sup>, and 4<sup>th</sup> member rings, triple bonds on the armchair edge are formed due to unsaturated carbons. Furthermore, one can see that the edge of the C<sub>24</sub> GND is armchair with two types of bond lengths (1.2380Å and 1.3890Å).

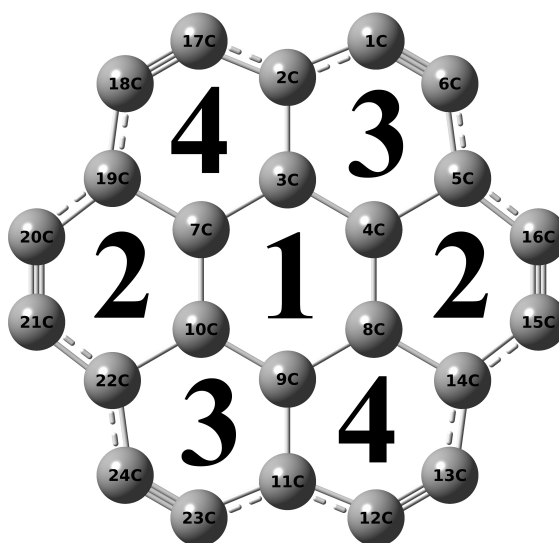


**Figure 3.2 Structure of C<sub>24</sub> graphene nano disk**

Member Ring	Bond length (angstrom)	Atom internal angle (degree)
1	3-4:	1.447648
	4-8:	1.447650
	8-9:	1.447648
	9-10:	1.447648
	10-7:	1.447650
	7-3:	1.447648
2	4-5/7-19:	1.488014
	5-16/19-20:	1.388999
	16-15/20-21:	1.237996
	15-14/21-22:	1.388999
	14-8/22-10:	1.488010
	8-4/10-7:	1.447650
3	2-1/11-23:	1.388998
	1-6/23-24:	1.237995
	6-5/24-22:	1.389000
	5-4/22-10:	1.488014
	4-3/10-9:	1.447648
	3-2/9-11:	1.488016
4	18-17/13-12:	1.237995
	17-2/12-11:	1.388998
	2-3/11-9:	1.488016
	3-7/9-8:	1.447648
	7-19/8-14:	1.488010
	19-18/14-13:	1.388999

If twelve new 6-member rings are formed around the edge of C24 GND, a larger concentric graphene nano disk (named as C54 GND) with 54 carbon atoms is created (Figure 3.3). Different from C24 GND that has only armchair edge, C54 GND possesses a hybrid edge of armchair and zigzag, namely, 6 edge-atoms are in the zigzag and 12 edge-atoms in the armchair. The bond length associated to a zigzag carbon atom is 1.4356Å, whereas the bond lengths of armchair carbons are 1.2510Å and 1.3919Å. There are 8 types of member rings in the C54 GND. In the central member ring, bond lengths decrease when compared with the smaller structure C24 GND, but the bond angle

remains unchanged due to its symmetrical structure. Furthermore, bond lengths in 2<sup>nd</sup>, 3<sup>rd</sup>, 4<sup>th</sup> member rings are different from those in C<sub>24</sub> GND. This happens because these member rings are not at the edge. The 5<sup>th</sup> and 7<sup>th</sup> member rings possess armchair edge with short C-C bond lengths between armchair carbons, whereas the 6<sup>th</sup> and 8<sup>th</sup> member rings have zigzag edge associated with longer bond lengths between zigzag edge carbons.

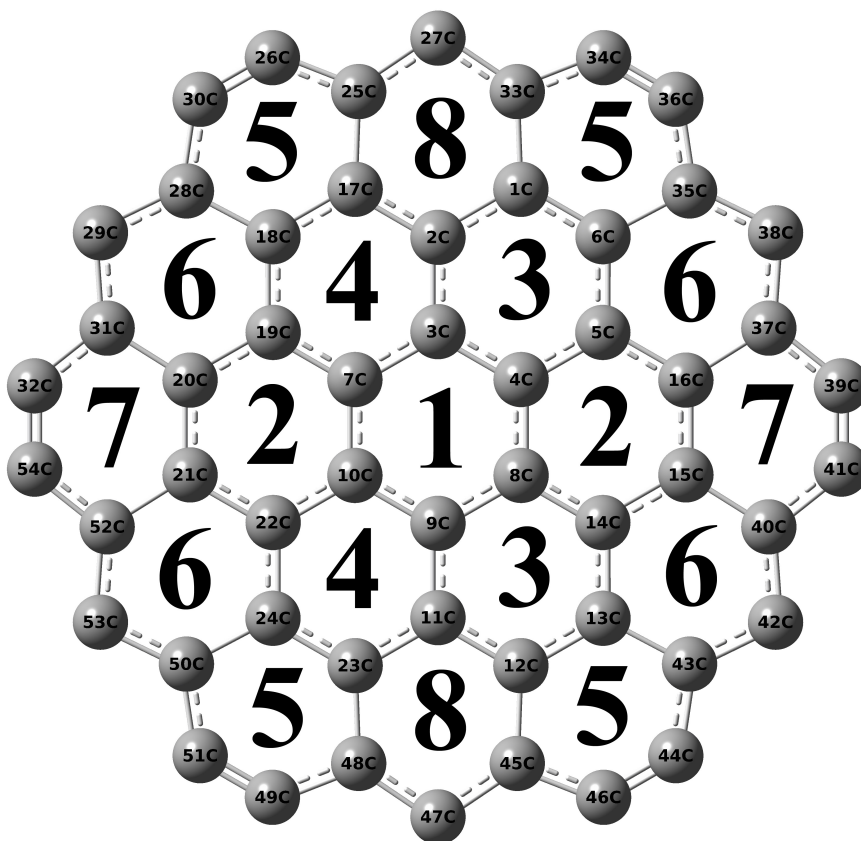


**Figure 3.3 Structure of C<sub>54</sub> graphene nano disk**

Member Ring	Bond length (angstrom)	Atom internal angle (degree)
1	3-4:	1.44005 3:
	4-8:	1.44005 4:
	8-9:	1.44005 8:
	9-10:	1.44005 9:
	10-7:	1.44006 10:
	7-3:	1.44005 7:
2	4-5/7-19:	1.41631 5/19:
	5-16/19-20:	1.43772 16/20:
	16-15/20-21:	1.42371 15/21:
	15-14/21-22:	1.43772 14/22:
	14-8/22-10:	1.41631 8/10:
	8-4/10-7:	1.44005 4/7:
3	2-1/11-23:	1.43772 1/23:
	1-6/23-24:	1.42371 6/24:
	6-5/24-22:	1.43772 5/22:
	5-4/22-10:	1.41631 4/10:
	4-3/10-9:	1.44005 3/9:
	3-2/9-11:	1.41631 2/11:
4	18-17/13-12:	1.42371 17/12:
	17-2/12-11:	1.43772 2/11:
	2-3/11-9:	1.41631 3/9:
	3-7/9-8:	1.44005 7/8:
	7-19/8-14:	1.41631 19/14:
	19-18/14-13:	1.43772 18/13:
5	25-26/33-34/43-44/48-49:	1.39186 26/34/46/49:
	26-30/34-36/44-46/49-51:	1.25098 30/36/44/51:
	30-28/36-35/46-45/51-50:	1.39186 28/35/43/50:
	28-18/35-6/45-12/50-24:	1.46958 18/6/13/24:
	18-17/6-1/12-13/24-23:	1.42371 17/1/12/23:
	17-25/1-33/13-43/23-48:	1.46958 25/33/45/48:
6	18-28/6-35/24-50/13-43:	1.46958 28/35/50/43:
	28-29/35-38/50-53/43-42:	1.43556 29/38/53/42:
	29-31/38-37/53-52/42-40:	1.43555 31/37/52/40:
	31-20/37-16/52-21/40-15:	1.46958 20/16/21/15:
	20-19/16-5/21-22/15-14:	1.43772 19/5/22/14:
	19-18/5-6/22-24/14-13:	1.43772 18/6/24/13:
7	16-37/20-31:	1.46958 37/31:
	37-39/31-32:	1.39186 39/32:
	39-41/32-54:	1.25098 41/54:
	41-40/54-52:	1.39186 40/52:
	40-15/52-21:	1.46958 15/21:
	15-16/21-20:	1.42371 16/20:
8	25-27/48-47:	1.43556 27/47:
	27-33/47-45:	1.43556 33/45:
	33-1/45-12:	1.46958 1/12:
	1-2/12-11:	1.43772 2/11:
	2-17/11-23:	1.43772 17/23:
	17-25/23-48:	1.46958 25/48:



When eighteen 6-member rings are formed around the edge of C54 GND, a new graphene nano disk (named as C96 GND) with 96 carbon atoms, is generated (Figure 3.4). In this large GND, 12 edge-atoms are in the armchair and 12 edge-atoms in zigzag. The bond lengths associated to a zigzag carbon atom are 1.3402Å and 1.3691Å, whereas the bond lengths of the armchair carbons are 1.2283Å and 1.4143Å. Furthermore, the short lengths (about 1.23Å) belong to the bonds formed between two nearest armchair-atoms. This occurs because armchair-atoms are unsaturated so that they can form triple bonds. The C96 GND consists of 13 types of member rings. For the 1<sup>st</sup> member ring through 8<sup>th</sup> member ring, all carbons are saturated. Furthermore, 9<sup>th</sup> to 13<sup>th</sup> member rings possess edge carbons. It should be noted that, in the central member ring (1<sup>st</sup> ring), the bond length increases from 1.3095Å to 1.4332Å when compared with C54 GND.

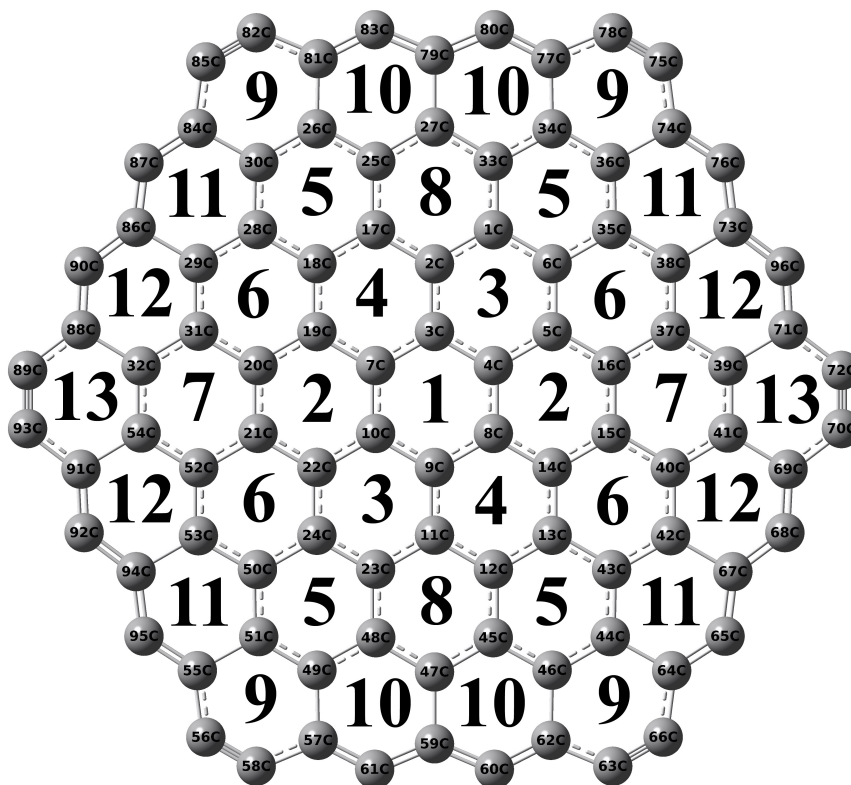


**Figure 3.4 Structure of C<sub>96</sub> graphene nano disk**

Member Ring	Bond length (angstrom)	Atom internal angle (degree)
1	3-4:	1.43322 3:
	4-8:	1.43322 4:
	8-9:	1.43322 8:
	9-10:	1.43322 9:
	10-7:	1.43322 10:
	7-3:	1.43322 7:
		120.00005
2	4-5/7-19:	1.43016 5/19:
	5-16/19-20:	1.43334 16/20:
	16-15/20-21:	1.43169 15/21:
	15-14/21-22:	1.43334 14/22:
	14-8/22-10:	1.43016 8/10:
	8-4/10-7:	1.43322 4/7:
		119.99997
3	2-1/11-23:	1.43334 1/23:
	1-6/23-24:	1.43169 6/24:
	6-5/24-22:	1.43334 5/22:
	5-4/22-10:	1.43016 4/10:
	4-3/10-9:	1.43322 3/9:
	3-2/9-11:	1.43322 2/11:
		120.03814
4	18-17/13-12:	1.43169 17/12:
	17-2/12-11:	1.43334 2/11:
	2-3/11-9:	1.43016 3/9:
	3-7/9-8:	1.43322 7/8:
	7-19/8-14:	1.43016 19/14:
	19-18/14-13:	1.43334 18/13:
		119.99997
5	25-26/33-34/43-44/48-49:	1.41842 26/34/46/49:
	26-30/34-36/44-46/49-51:	1.41594 30/36/44/51:
	30-28/36-35/46-45/51-50:	1.41842 28/35/43/50:
	28-18/35-6/45-12/50-24:	1.44420 18/6/13/24:
	18-17/6-1/12-13/24-23:	1.43169 17/1/12/23:
	17-25/1-33/13-43/23-48:	1.44420 25/33/45/48:
		118.72399
6	18-28/6-35/24-50/13-43:	1.44420 28/35/50/43:
	28-29/35-38/50-53/43-42:	1.43427 29/38/53/42:
	29-31/38-37/53-52/42-40:	1.43427 31/37/52/40:
	31-20/37-16/52-21/40-15:	1.44420 20/16/21/15:
	20-19/16-5/21-22/15-14:	1.43334 19/5/22/14:
	19-18/5-6/22-24/14-13:	1.43334 18/6/24/13:
		119.92374
7	16-37/20-31:	1.44420 37/31:
	37-39/31-32:	1.41842 39/32:
	39-41/32-54:	1.41595 41/54:
	41-40/54-52:	1.41842 40/52:
	40-15/52-21:	1.44420 15/21:
	15-16/21-20:	1.43169 16/20:
		120.14922
8	25-27/48-47:	1.43427 27/47:
	27-33/47-45:	1.43427 33/45:
	33-1/45-12:	1.44420 1/12:
	1-2/12-11:	1.43334 2/11:
	2-17/11-23:	1.43334 17/23:
	17-25/23-48:	1.44420 25/48:
		119.88886

Member Ring	Bond length (angstrom)		Atom internal angle (degree)	
9	77-78/81-82/55-56/64-66:	1.41429	78/82/58/63:	126.94822
	78-75/82-85/56-58/66-63:	1.22827	75/85/57/66:	126.94819
	75-74/85-84/58-57/63-62:	1.41429	74/84/49/64:	112.12461
	74-36/84-30/57-49/62-46:	1.47151	36/30/51/44:	120.92716
	36-34/30-26/49-51/46-44:	1.41594	34/26/55/46:	120.92722
	34-77/26-81/51-55/44-64:	1.47151	77/81/56/62:	112.12459
10	81-83/77-80/57-61/62-60:	1.34025	81/77/57/62:	117.94603
	83-79/80-79/61-59/60-59:	1.36912	83/80/61/60:	130.09995
	79-27/79-27/59-47/59-47:	1.50695	79/79/59/59:	112.88121
	27-25/27-33/47-48/47-45:	1.43427	27/27/47/47:	120.40055
	25-26/33-34/48-49/45-46:	1.41842	25/33/48/45:	120.72625
	26-81/34-77/49-57/46-62:	1.47151	26/34/49/46:	117.94600
11	36-74/30-84/51-55/44-64:	1.47151	36/30/51/44:	117.94603
	74-76/84-87/55-95/64-65:	1.34025	74/84/55/64:	117.94600
	76-73/87-86/95-94/65-67:	1.36912	76/87/95/65:	130.09995
	73-38/86-29/94-53/67-42:	1.50695	73/86/94/67:	112.88124
	38-35/29-28/53-50/42-43:	1.43427	38/29/53/42:	120.40060
	35-36/28-30/50-51/43-44:	1.41842	35/28/50/43:	120.72617
12	38-73/29-86/53-94/42-67:	1.50695	38/29/53/42:	120.40061
	73-96/86-90/94-92/67-68:	1.36912	73/86/94/67:	112.88118
	96-71/90-88/92-91/68-697:	1.34025	95/90/92/68:	130.10001
	71-39/88-32/91-54/69-41:	1.47151	71/88/91/69:	117.94596
	39-37/32-31/54-52/41-40:	1.41842	39/32/54/54:	117.94608
	37-38/31-29/52-53/40-42:	1.43427	37/31/52/52	120.72616
13	39-71/32-88:	1.47151	39/32:	120.92716
	71-72/88-89:	1.41429	71/88:	112.12461
	72-70/89-93:	1.22827	72/89:	126.94822
	70-69/93-91:	1.41429	70/93:	126.94822
	69-41/91-54:	1.47151	69/91:	112.12461
	41-39/54-32:	1.41595	41/54:	120.92716

From the above discussion, one can see that, for a concentric graphene nano disk, there are 12 armchair-edge-atoms, which is independent on the size of the disk, whereas the number of zigzag-edge-atoms increases with increasing the size of the disk. As a result, when the size of a graphene nano disk increases, the zigzag-edge of a graphene nano disk becomes dominant.

### 3.2 Stability of graphene nano disks

To examine the stability of a graphene nano disk, we calculated the stabilization energy by using the following equation:

$$E_{st} = \frac{E_{Graphene} - n \times E_C}{n} \quad (6)$$

Where  $E_{st}$ ,  $E_{graphene}$ , and  $E_C$  are stabilization energy of graphene, system energy of graphene, and energy of a carbon atom, which were obtained from B3lyp calculations. The  $n$  is the number of carbon atoms contained in a graphene nano disk (GND). As shown in Figure 3.5, one can see that the stabilization energy increases with increasing the number of carbon atoms in GNDs. However, the increase of the energy is small from C54 to C96 GND. This indicates that the larger the graphene nano disk, the more stable it is. Different from a large graphene sheet, a nano disk has a large ratio of unsaturated carbon atoms to saturated ones. The ratio decreases with increasing size of a graphene nano disk. Because unsaturated carbons are instable, the decrease in the ratio of unsaturated carbons to saturated ones could increase the stability of the graphene nano disk. Therefore, one can conclude that the larger the disk, the more favorable the formation of the disk is.

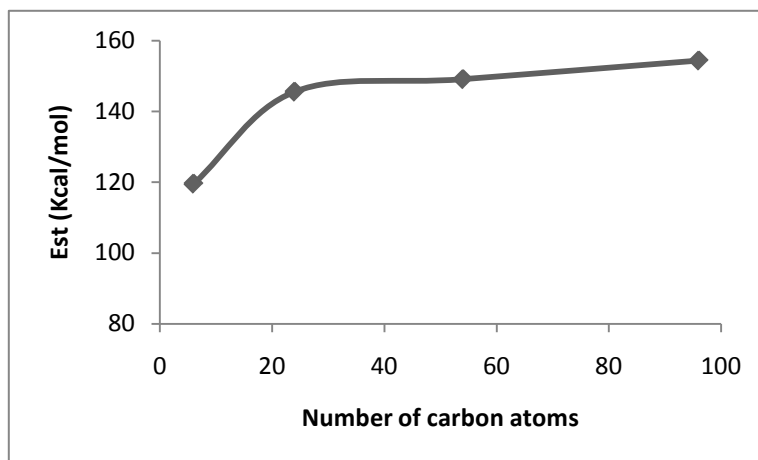


**Figure 3.5 Stabilization energy ( $E_{st}$ ) of graphene vs. its number of carbon atoms.**

### ***3.3 HOMO-LUMO energy gaps of graphene nano disks***

The conductance of a macro molecule is determined by its energy gap between the highest occupied molecular orbital (HOMO) and the lowest unoccupied molecular orbital (LUMO) (56, 57). It is well-known that the smaller HOMO-LUMO gap favors a higher conductance. In general, if the energy gap is greater than 5eV, electrons are difficult to move. In contrast, the realization of “charge transfer” between HOMO and LUMO bands requires that the HOMO-LUMO energy gap must be small compared with the band width. Since the band width for an ordinary organic metal is about 0.5-1eV, the HOMO-LUMO energy gap must be less than 0.5eV (60). Therefore, a material with the energy gap larger than 5eV is defined as an insulator, whereas one with the energy gap smaller than 0.5eV is called as a conductor. Furthermore, a material with the energy gap between 0.5 and 3.5eV is defined as a semiconductor. It would be important to examine how the size of a graphene nano disk affects its HOMO-LUMO energy gap, which can

allow us to evaluate its conductance. As shown in Figure 3.6, one can see that C6 and C24 GNDs have HOMO-LUMO gaps of 1.7 and 2.1eV, respectively. This indicates that C6 and C24 GNDs are semi-conductors. However, the HOMO-LUMO gap of C54 and C96 GNDs are about 0.3eV, indicating that they are organic metals. Therefore, a larger graphene nano disk has higher electrical conductance than a smaller one, because the electrical conductance of a macro molecule is reversely proportional to its HOMO-LUMO energy gap.

The electronic properties of graphene nano disk are size dependent, which is similar with the case in graphene nanoribbons (GNRs) (61, 62). GNRs show distinct electrical properties for different edge shapes and widths. GNRs can be divided to two types: armchair graphene nanoribbons (AGNRs) and zigzag graphene nanoribbons (ZGNRs). AGNRs are either semiconducting or metallic which depending on their width, whereas ZGNRs are always metallic independent on their widths (62).

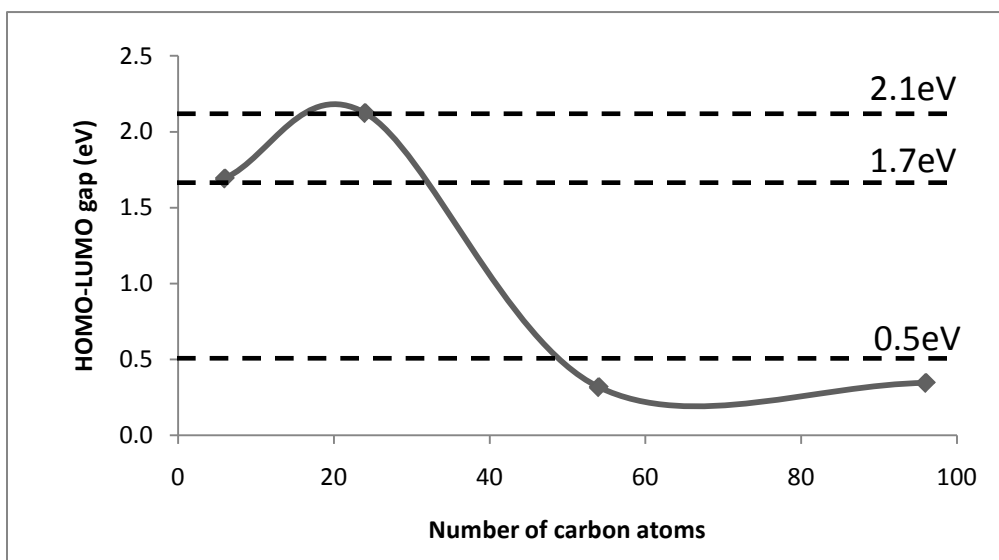


**Figure 3.6 HOMO-LUMO energy gaps of graphene nano disks vs. the number of carbon atoms**

## Chapter 4

### Structures and Properties of Graphene Nano Disks (GND) with Edge-doping

To reveal the effect of edge-doping on the structures and the properties of graphene nano disks, the geometries and energies of the disks doped with H, Li, OH, and F at their edges were evaluated by B3lyp and Pw91pw91 DFT calculations.

#### *4.1 Structures of graphene nano disks with edge-dopants*

When we saturate the smallest graphene nano disk (C6 GND) by H atom, we can obtain a benzene structure, in which the bond angle ( $120^\circ$ ) of each carbon remains unchanged, but the C-C bond lengths increases from 1.3096 to 1.3965Å (Figure 4.1). This is in excellent agreement with experimental value (1.40Å). When a H-atom is attached to each of edge carbon atoms of C24 GND, the bond lengths of carbon to carbon increase from 1.2370Å and 1.3890Å to 1.3723Å and 1.4240Å, respectively (Figure 4.2). If the each edge-carbon-atom of C54 GND is saturated by H atom, the bond lengths associated to armchair-edge carbons increase from 1.2510 and 1.3919Å to 1.3632 and 1.4372Å, respectively (Figure 4.3). The bond lengths associated to zigzag-edge carbons decreased from 1.4356 to 1.4013Å, respectively. When 18 H atoms are attached to the edge of C96 GND, the bond lengths associated to a zigzag-edge carbon atom increase from 1.3402 and 1.3691Å to 1.3900 and 1.4163Å, and the bond lengths of armchair carbons also increase from 1.2283 and 1.4143Å to 1.3591 and 1.4432Å (Figure 4.4). The increase of bond length can be easily understood, because the attached H atom forms a

bond with its contacting C, so that the binding ability of the carbon to other carbons decreases. The similar structure changes can be observed for F and OH-doped graphene nano disks (Figure 4.5 and 4.8). However, if Li atom is employed to saturate C6 GND, although the bond lengths are subjected to the similar changes as H, F, or OH-doped GNDs, the bond angles of carbons changed from  $120^\circ$  to two angles  $109.9$  and  $140.2^\circ$ , indicated a shape change (Figure 4.12). Furthermore, when Li atoms are attached to the C24 GND (Figure 4.13), its structure is the similar to those of H, F, or OH-doped C24 GNDs. However, Li-doped C54 GND possesses a different structure, in which some bonds between Li and Li are formed (Figure 4.14).

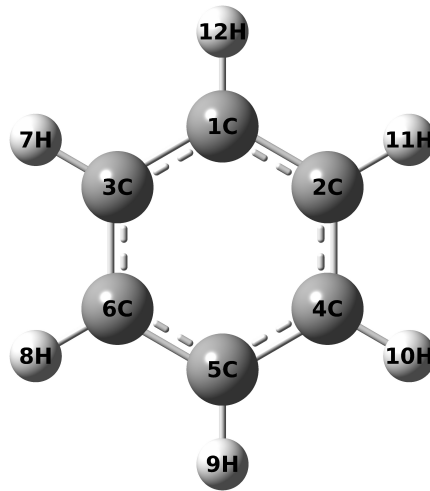


***Figure 4.1 Structure of  $C_6$  graphene nano disk with H-dopants***

Bond length (angstrom)		Atom internal angle (degree)	
1-2:	1.39648	1:	119.99993
2-4:	1.39648	2:	120.00003
4-5:	1.39648	4:	120.00003
5-6:	1.39648	5:	119.99993
6-3:	1.39648	6:	120.00003
3-1:	1.39648	3:	120.00003



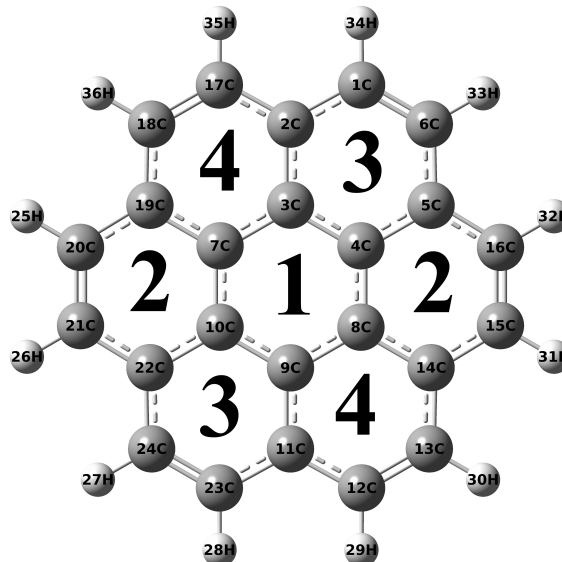


***Figure 4.2 Structure of  $C_{24}$  graphene nano disk with H-dopants***

Member Ring	Bond length (angstrom)		Atom internal angle (degree)	
1	3-4:	1.42750	3:	120.00005
	4-8:	1.42750	4:	119.99998
	8-9:	1.42750	8:	119.99998
	9-10:	1.42750	9:	120.00005
	10-7:	1.42750	10:	119.99998
	7-3:	1.42750	7:	119.99998
	4-5/7-19:	1.42156	5/19:	118.76800
2	5-16/19-20:	1.42401	16/20:	121.23202
	16-15/20-21:	1.37234	15/21:	121.23202
	15-14/21-22:	1.42401	14/22:	118.76800
	14-8/22-10:	1.42156	8/10:	119.99998
	8-4/10-7:	1.42750	4/7:	119.99998
	2-1/11-23:	1.42401	1/23:	121.23204
	1-6/23-24:	1.37234	6/24:	121.23202
3	6-5/24-22:	1.42401	5/22:	118.76796
	5-4/22-10:	1.42156	4/10:	120.00004
	4-3/10-9:	1.42750	3/9:	119.99998
	3-2/9-11:	1.42156	2/11:	118.76797
	18-17/13-12:	1.37234	17/12:	121.23204
	17-2/12-11:	1.42401	2/11:	118.76797
	2-3/11-9:	1.42156	3/9:	119.99998
4	3-7/9-8:	1.42750	7/8:	120.00004
	7-19/8-14:	1.42156	19/14:	118.76796
	19-18/14-13:	1.42401	18/13:	121.23202

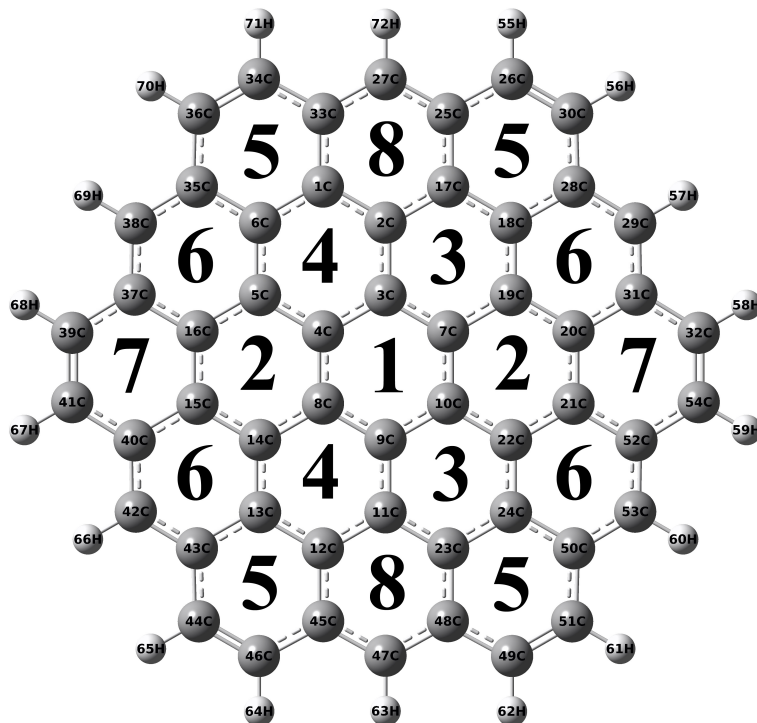


***Figure 4.3 Structure of  $C_{54}$  graphene nano disk with H-dopants***

Member Ring	Bond length (angstrom)		Atom internal angle (degree)	
1	3-4:	1.41959	3:	120.00209
	4-8:	1.41961	4:	119.99582
	8-9:	1.41959	8:	120.00209
	9-10:	1.41959	9:	120.00209
	10-7:	1.41961	10:	119.99582
	7-3:	1.41959	7:	120.00209
	4-5/7-19:	1.42916	5/19:	119.94356
2	5-16/19-20:	1.42037	16/20:	120.05414
	16-15/20-21:	1.42618	15/21:	120.05414
	15-14/21-22:	1.42037	14/22:	119.94356
	14-8/22-10:	1.42916	8/10:	120.00229
	8-4/10-7:	1.41961	4/7:	120.00229
	2-1/11-23:	1.42036	1/23:	120.04786
	1-6/23-24:	1.42616	6/24:	120.05374
3	6-5/24-22:	1.42038	5/22:	119.95030
	5-4/22-10:	1.42916	4/10:	119.99561
	4-3/10-9:	1.41959	3/9:	120.00209
	3-2/9-11:	1.42918	2/11:	119.95040

Member Ring	Bond length (angstrom)		Atom internal angle (degree)	
4	18-17/13-12:	1.42616	17/12:	120.04786
	17-2/12-11:	1.42036	2/11:	119.95040
	2-3/11-9:	1.42918	3/9:	120.00209
	3-7/9-8:	1.41959	7/8:	119.99561
	7-19/8-14:	1.42916	19/14:	119.95030
	19-18/14-13:	1.42038	18/13:	120.05374
5	25-26/33-34/43-44/48-49:	1.43723	26/34/46/49:	121.51776
	26-30/34-36/44-46/49-51:	1.36317	30/36/44/51:	121.52148
	30-28/36-35/46-45/51-50:	1.43723	28/35/43/50:	118.26697
	28-18/35-6/45-12/50-24:	1.43049	18/6/13/24:	120.21196
	18-17/6-1/12-13/24-23:	1.42616	17/1/12/23:	120.21626
	17-25/1-33/13-43/23-48:	1.43051	25/33/45/48:	118.26557
6	18-28/6-35/24-50/13-43:	1.43049	28/35/50/43:	119.73430
	28-29/35-38/50-53/43-42:	1.40133	29/38/53/42:	121.95561
	29-31/38-37/53-52/42-40:	1.40131	31/37/52/40:	119.24053
	31-20/37-16/52-21/40-15:	1.43050	20/16/21/15:	119.72877
	20-19/16-5/21-22/15-14:	1.42037	19/5/22/14:	120.10614
	19-18/5-6/22-24/14-13:	1.42038	18/6/24/13:	119.73430
7	16-37/20-31:	1.43050	37/31:	118.26009
	37-39/31-32:	1.43725	39/32:	121.52282
	39-41/32-54:	1.36316	41/54:	121.52282
	41-40/54-52:	1.43725	40/52:	118.26009
	40-15/52-21:	1.43050	15/21:	120.21709
	15-16/21-20:	1.42618	16/20:	120.21709
8	25-27/48-47:	1.40133	27/47:	121.94841
	27-33/47-45:	1.40133	33/45:	119.24032
	33-1/45-12:	1.43051	1/12:	119.73588
	1-2/12-11:	1.42036	2/11:	120.09920
	2-17/11-23:	1.42036	17/23:	119.73588
	17-25/23-48:	1.43051	25/48:	119.24032

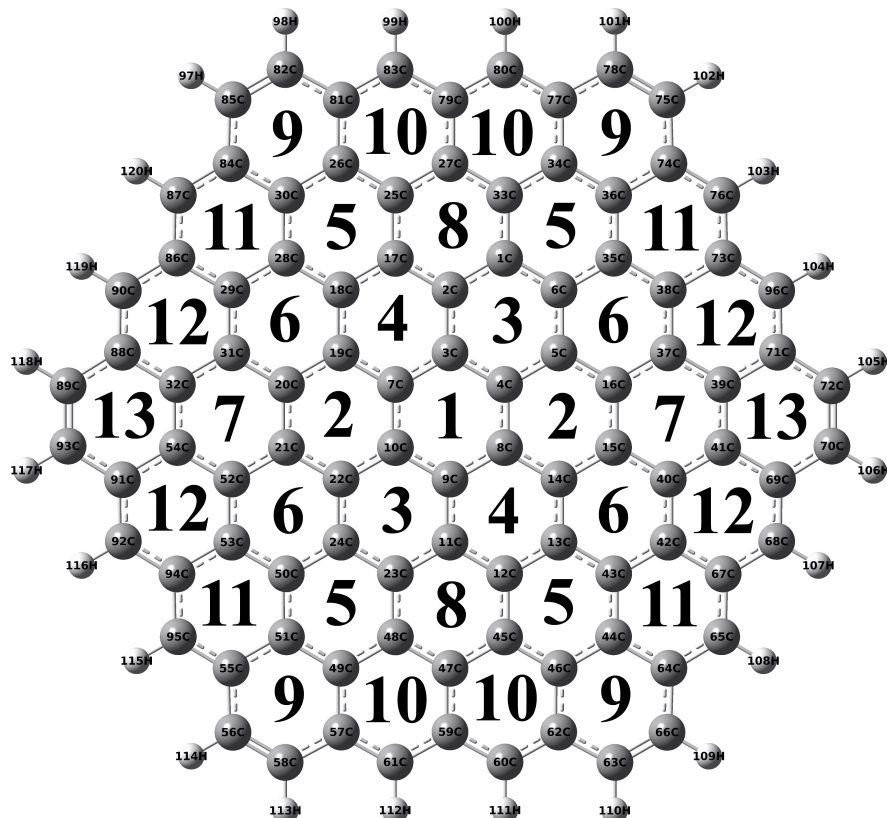


***Figure 4.4 Structure of  $C_{96}$  graphene nano disk with H-dopants***

Member	Ring	Bond length (angstrom)		Atom internal angle (degree)	
1	3-4:	1.42358	3:	119.99517	
	4-8:	1.42360	4:	120.00241	
	8-9:	1.42358	8:	120.00241	
	9-10:	1.42358	9:	119.99517	
	10-7:	1.42360	10:	120.00241	
	7-3:	1.42358	7:	120.00241	
2	4-5/7-19:	1.41965	5/19:	119.95305	
	5-16/19-20:	1.42399	16/20:	120.04457	
	16-15/20-21:	1.41745	15/21:	120.04457	
	15-14/21-22:	1.42399	14/22:	120.00238	
	14-8/22-10:	1.41965	8/10:	120.00238	
	8-4/10-7:	1.42360	4/7:	120.00238	

Member Ring	Bond length (angstrom)	Atom internal angle (degree)
3	2-1/11-23:	1.42399 1/23: 120.03741
	1-6/23-24:	1.41743 6/24: 120.04468
	6-5/24-22:	1.42401 5/22: 119.96009
	5-4/22-10:	1.41965 4/10: 119.99520
	4-3/10-9:	1.42358 3/9: 120.00241
	3-2/9-11:	1.41967 2/11: 119.96020
4	18-17/13-12:	1.41743 17/12: 120.03741
	17-2/12-11:	1.42399 2/11: 119.96020
	2-3/11-9:	1.41967 3/9: 120.00241
	3-7/9-8:	1.42358 7/8: 119.99520
	7-19/8-14:	1.41965 19/14: 119.96009
	19-18/14-13:	1.42401 18/13: 120.04468
5	25-26/33-34/43-44/48-49:	1.42002 26/34/46/49: 120.11587
	26-30/34-36/44-46/49-51:	1.42100 30/36/44/51: 120.12132
	30-28/36-35/46-45/51-50:	1.42005 28/35/43/50: 119.85997
	28-18/35-6/45-12/50-24:	1.42774 18/6/13/24: 120.01825
	18-17/6-1/12-13/24-23:	1.41743 17/1/12/23: 120.02531
	17-25/1-33/13-43/23-48:	1.42776 25/33/45/48: 119.85929
6	18-28/6-35/24-50/13-43:	1.42774 28/35/50/43: 119.93610
	28-29/35-38/50-53/43-42:	1.42276 29/38/53/42: 120.16674
	29-31/38-37/53-52/42-40:	1.42278 31/37/52/40: 119.94288
	31-20/37-16/52-21/40-15:	1.42774 20/16/21/15: 119.93035
	20-19/16-5/21-22/15-14:	1.42399 19/5/22/14: 120.08686
	19-18/5-6/22-24/14-13:	1.42401 18/6/24/13: 119.93707
7	16-37/20-31:	1.42774 37/31: 119.85310
	37-39/31-32:	1.42004 39/32: 120.12183
	39-41/32-54:	1.42100 41/54: 120.12183
	41-40/54-52:	1.42004 40/52: 119.85310
	40-15/52-21:	1.42774 15/21: 120.02508
	15-16/21-20:	1.41745 16/20: 120.02508
8	25-27/48-47:	1.42276 27/47: 120.15907
	27-33/47-45:	1.42276 33/45: 119.94338
	33-1/45-12:	1.42776 1/12: 119.93729
	1-2/12-11:	1.42399 2/11: 120.07960
	2-17/11-23:	1.42399 17/23: 119.93729
	17-25/23-48:	1.42776 25/48: 119.94338

Member Ring	Bond length (angstrom)		Atom internal angle (degree)	
9	77-78/81-82/55-56/64-66:	1.44318	78/82/58/63:	121.66470
	78-75/82-85/56-58/66-63:	1.35910	75/85/57/66:	121.66784
	75-74/85-84/58-57/63-62:	1.44317	74/84/49/64:	117.98788
	74-36/84-30/57-49/62-46:	1.43830	36/30/51/44:	120.34484
	36-34/30-26/49-51/46-44:	1.42100	34/26/55/46:	120.34818
	34-77/26-81/51-55/44-64:	1.43832	77/81/56/62:	117.98656
10	81-83/77-80/57-61/62-60:	1.39001	81/77/57/62:	119.52095
	83-79/80-79/61-59/60-59:	1.41633	83/80/61/60:	122.09779
	79-27/79-27/59-47/59-47:	1.43295	79/79/59/59:	118.72751
	27-25/27-33/47-48/47-45:	1.42276	27/27/47/47:	119.92047
	25-26/33-34/48-49/45-46:	1.42002	25/33/48/45:	120.19733
	26-81/34-77/49-57/46-62:	1.43832	26/34/49/46:	119.53595
11	36-74/30-84/51-55/44-64:	1.43830	36/30/51/44:	119.53385
	74-76/84-87/55-95/64-65:	1.39002	74/84/55/64:	119.51576
	76-73/87-86/95-94/65-67:	1.41631	76/87/95/65:	122.10397
	73-38/86-29/94-53/67-42:	1.43291	73/86/94/67:	118.72858
	38-35/29-28/53-50/42-43:	1.42276	38/29/53/42:	119.91391
	35-36/28-30/50-51/43-44:	1.42005	35/28/50/43:	120.20394
12	38-73/29-86/53-94/42-67:	1.43291	38/29/53/42:	119.91935
	73-96/86-90/94-92/67-68:	1.41633	73/86/94/67:	118.72226
	96-71/90-88/92-91/68-69:	1.38999	96/90/92/68:	122.10455
	71-39/88-32/91-54/69-41:	1.43831	71/88/91/69:	119.52137
	39-37/32-31/54-52/41-40:	1.42004	39/32/54/54:	119.52846
	37-38/31-29/52-53/40-42:	1.42278	37/31/52/52:	120.20402
13	39-71/32-88:	1.43831	39/32:	120.34971
	71-72/88-89:	1.44319	71/88:	117.98067
	72-70/89-93:	1.35908	72/89:	121.66962
	70-69/93-91:	1.44319	70/93:	121.66962
	69-41/91-54:	1.43831	69/91:	117.98067
	41-39/54-32:	1.42100	41/54:	120.34971

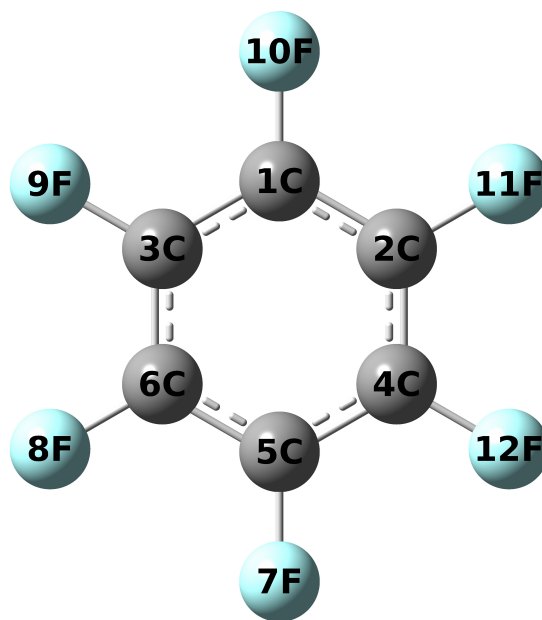


***Figure 4.5 Structure of  $C_6$  graphene nano disk with F-dopants***

Bond length (angstrom)		Atom internal angle (degree)	
1-2:	1.3935758	1:	119.9999910
2-4:	1.3953576	2:	120.0000045
4-5:	1.3935758	4:	119.9999910
5-6:	1.3935758	5:	120.0000045
6-3:	1.3953576	6:	119.9999910
3-1:	1.3935758	3:	119.9999910

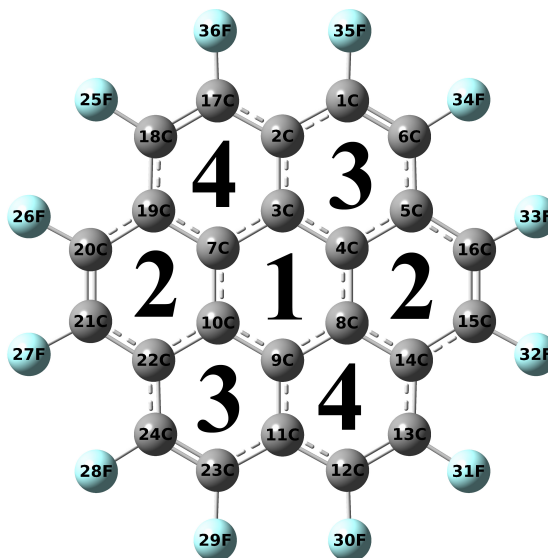


***Figure 4.6 Structure of  $C_{24}$  graphene nano disk with F-dopants***

Member Ring	Bond length (angstrom)	Atom internal angle (degree)
1	3-4:	1.42862
	3:	119.99994
	4-8:	1.42862
	4:	120.00003
	8-9:	1.42862
	8:	120.00003
	9-10:	1.42862
2	9:	119.99994
	10-7:	1.42862
	10:	120.00003
	7-3:	1.42862
	7:	120.00003
	4-5/7-19:	1.42563
	5/19:	118.49123
3	5-16/19-20:	1.41822
	16/20:	121.50876
	16-15/20-21:	1.37185
	15/21:	121.50876
	15-14/21-22:	1.41822
	14/22:	118.49123
	14-8/22-10:	1.42563
4	8/10:	120.00001
	8-4/10-7:	1.42862
	4/7:	120.00001
	2-1/11-23:	1.41822
	1/23:	121.50876
	1-6/23-24:	1.37185
	6/24:	121.50873
	6-5/24-22:	1.41822
	5/22:	118.49126
	5-4/22-10:	1.42563
	4/10:	119.99997
	4-3/10-9:	1.42862
	3/9:	120.00003
	3-2/9-11:	1.42563
	2/11:	118.49125
	18-17/13-12:	1.37185
	17/12:	121.50876
	17-2/12-11:	1.41822
	2/11:	118.49125
	2-3/11-9:	1.42563
	3/9:	120.00003
	3-7/9-8:	1.42862
	7/8:	119.99997
	7-19/8-14:	1.42563
	19/14:	118.49126
	19-18/14-13:	1.41822
	18/13:	121.50873



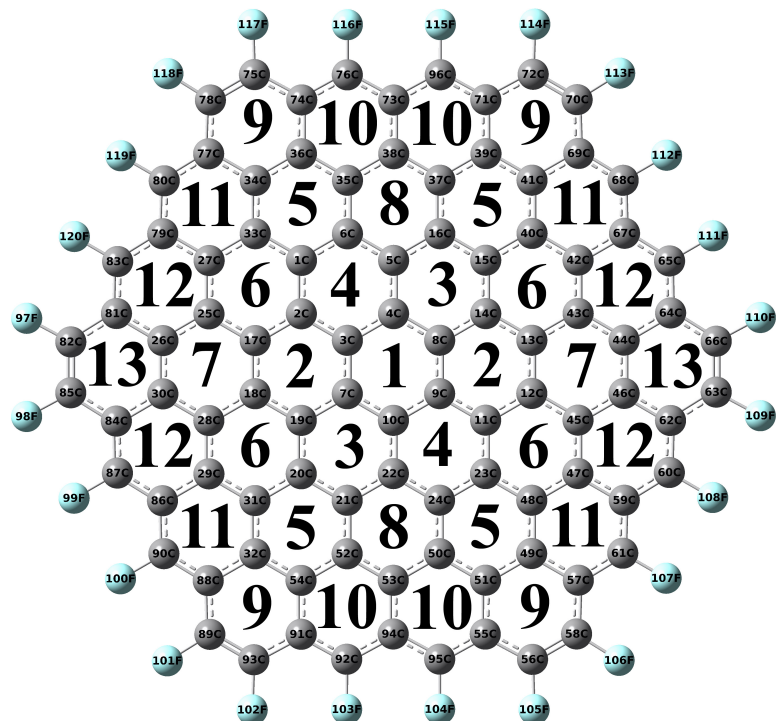


***Figure 4.7 Structure of  $C_{96}$  graphene nano disk with F-dopants***

Member Ring	Bond length (angstrom)		Atom internal angle (degree)	
1	3-4:	1.42498	3:	119.99433
	4-8:	1.42500	4:	120.00284
	8-9:	1.42498	8:	120.00284
	9-10:	1.42498	9:	119.99433
	10-7:	1.42500	10:	120.00284
	7-3:	1.42498	7:	120.00284
	4-5/7-19:	1.42128	5/19:	119.95036
2	5-16/19-20:	1.42527	16/20:	120.04773
	16-15/20-21:	1.41903	15/21:	120.04773
	15-14/21-22:	1.42527	14/22:	119.95036
	14-8/22-10:	1.42128	8/10:	120.00191
	8-4/10-7:	1.42500	4/7:	120.00191
	2-1/11-23:	1.42525	1/23:	120.03914
3	1-6/23-24:	1.41903	6/24:	120.05085
	6-5/24-22:	1.42527	5/22:	119.95520
	5-4/22-10:	1.42128	4/10:	119.99525
	4-3/10-9:	1.42498	3/9:	120.00284
	3-2/9-11:	1.42132	2/11:	119.95671

Member Ring	Bond length (angstrom)		Atom internal angle (degree)	
4	18-17/13-12:	1.41903	17/12:	120.03914
	17-2/12-11:	1.42525	2/11:	119.95671
	2-3/11-9:	1.42132	3/9:	120.00284
	3-7/9-8:	1.42498	7/8:	119.99525
	7-19/8-14:	1.42128	19/14:	119.95520
	19-18/14-13:	1.42527	18/13:	120.05085
5	25-26/33-34/43-44/48-49:	1.42180	26/34/46/49:	120.08666
	26-30/34-36/44-46/49-51:	1.42183	30/36/44/51:	120.10110
	30-28/36-35/46-45/51-50:	1.42181	28/35/43/50:	119.90334
	28-18/35-6/45-12/50-24:	1.42850	18/6/13/24:	119.99769
	18-17/6-1/12-13/24-23:	1.41903	17/1/12/23:	120.00715
	17-25/1-33/13-43/23-48:	1.42857	25/33/45/48:	119.90406
6	18-28/6-35/24-50/13-43:	1.42850	28/35/50/43:	119.86648
	28-29/35-38/50-53/43-42:	1.42394	29/38/53/42:	120.27027
	29-31/38-37/53-52/42-40:	1.42392	31/37/52/40:	119.86888
	31-20/37-16/52-21/40-15:	1.42853	20/16/21/15:	119.94847
	20-19/16-5/21-22/15-14:	1.42527	19/5/22/14:	120.09444
	19-18/5-6/22-24/14-13:	1.42527	18/6/24/13:	119.95145
7	16-37/20-31:	1.42853	37/31:	119.90134
	37-39/31-32:	1.42184	39/32:	120.09486
	39-41/32-54:	1.42181	41/54:	120.09486
	41-40/54-52:	1.42184	40/52:	119.90134
	40-15/52-21:	1.42853	15/21:	120.00380
	15-16/21-20:	1.41903	16/20:	120.00380
8	25-27/48-47:	1.42392	27/47:	120.26003
	27-33/47-45:	1.42392	33/45:	119.87299
	33-1/45-12:	1.42857	1/12:	119.95370
	1-2/12-11:	1.42525	2/11:	120.08657
	2-17/11-23:	1.42525	17/23:	119.95370
	17-25/23-48:	1.42857	25/48:	119.87299
9	77-78/81-82/55-56/64-66:	1.43597	78/82/58/63:	121.81466
	78-75/82-85/56-58/66-63:	1.35819	75/85/57/66:	121.83586
	75-74/85-84/58-57/63-62:	1.43587	74/84/49/64:	117.91072
	74-36/84-30/57-49/62-46:	1.43921	36/30/51/44:	120.26004
	36-34/30-26/49-51/46-44:	1.42183	34/26/55/46:	120.26937
	34-77/26-81/51-55/44-64:	1.43931	77/81/56/62:	117.90935
10	81-83/77-80/57-61/62-60:	1.38823	81/77/57/62:	119.01682
	83-79/80-79/61-59/60-59:	1.41424	83/80/61/60:	122.80714
	79-27/79-27/59-47/59-47:	1.43334	79/79/59/59:	118.43913
	27-25/27-33/47-48/47-45:	1.42392	27/27/47/47:	119.86998
	25-26/33-34/48-49/45-46:	1.42180	25/33/48/45:	120.22295
	26-81/34-77/49-57/46-62:	1.43931	26/34/49/46:	119.64397

Member Ring	Bond length (angstrom)		Atom internal angle (degree)	
11	36-74/30-84/51-55/44-64:	1.43921	36/30/51/44:	119.63886
	74-76/84-87/55-95/64-65:	1.38828	74/84/55/64:	119.01718
	76-73/87-86/95-94/65-67:	1.41419	76/87/95/65:	122.80859
	73-38/86-29/94-53/67-42:	1.43327	73/86/94/67:	118.44131
	38-35/29-28/53-50/42-43:	1.42394	38/29/53/42:	119.86388
	35-36/28-30/50-51/43-44:	1.42181	35/28/50/43:	120.23017
12	38-73/29-86/53-94/42-67:	1.43327	38/29/53/42:	119.86585
	73-96/86-90/94-92/67-68:	1.41428	73/86/94/67:	118.43934
	96-71/90-88/92-91/68-69:	1.38820	96/90/92/68:	122.81057
	71-39/88-32/91-54/69-41:	1.43930	71/88/91/69:	119.01548
	39-37/32-31/54-52/41-40:	1.42184	39/32/54/54:	119.63898
	37-38/31-29/52-53/40-42:	1.42392	37/31/52/52:	120.22978
13	39-71/32-88:	1.43930	39/32:	120.26616
	71-72/88-89:	1.43602	71/88:	117.90945
	72-70/89-93:	1.35820	72/89:	121.82439
	70-69/93-91:	1.43602	70/93:	121.82439
	69-41/91-54:	1.43930	69/91:	117.90945
	41-39/54-32:	1.42181	41/54:	120.26616

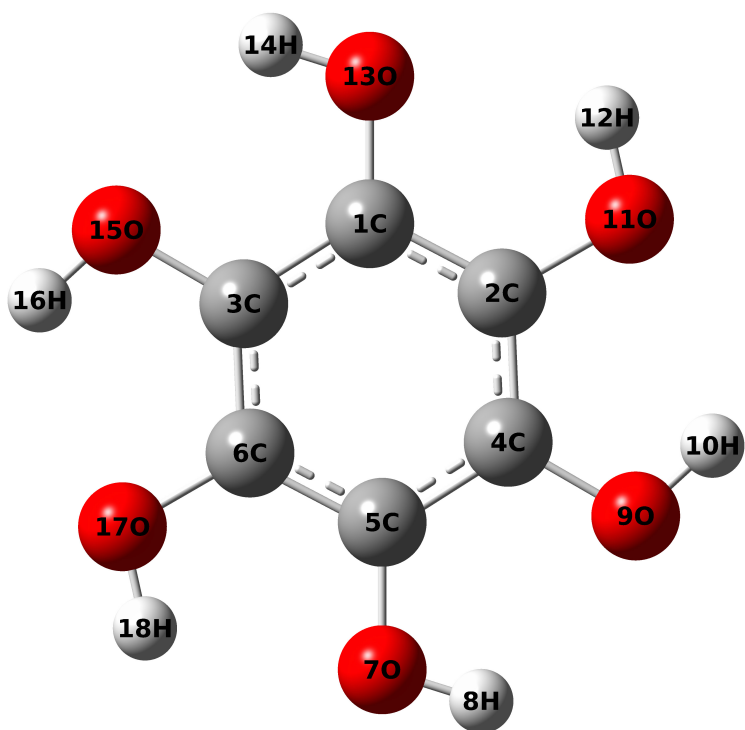


***Figure 4.8 Structure of  $C_6$  graphene nano disk with OH-dopants***

Bond length (angstrom)		Atom internal angle (degree)	
1-2:	1.3949046	1:	119.9951297
2-4:	1.3948918	2:	120.0003034
4-5:	1.3948918	4:	120.0045773
5-6:	1.39491	5:	119.9951747
6-3:	1.3948904	6:	120.0001926
3-1:	1.3948850	3:	120.004623

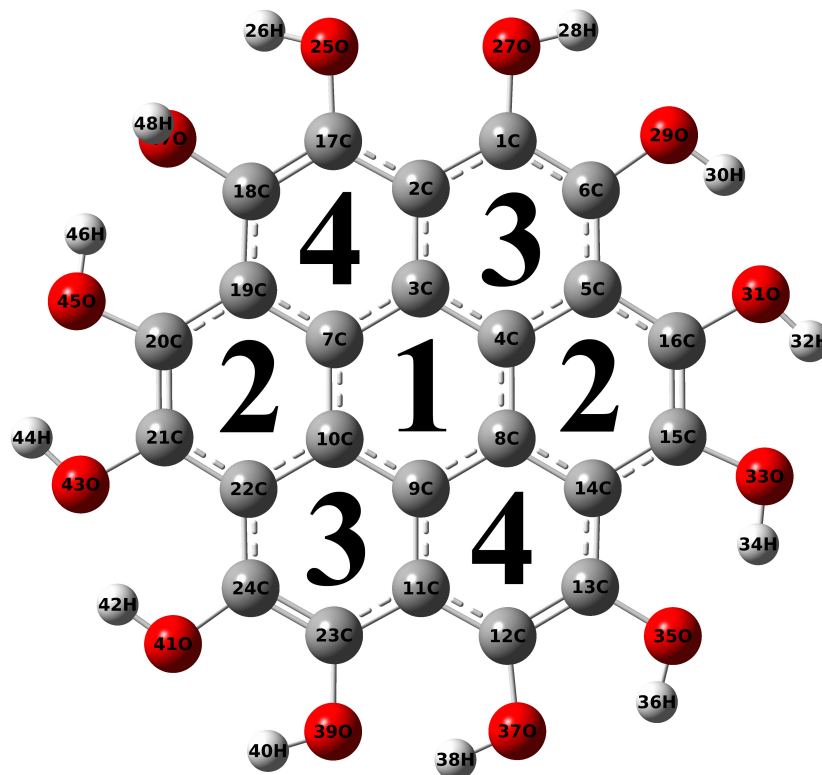


***Figure 4.9 Structure of  $C_{24}$  graphene nano disk with OH-dopants***

Member Ring	Bond length (angstrom)		Atom internal angle (degree)	
1	3-4:	1.42882	3:	119.18744
	4-8:	1.43021	4:	120.41749
	8-9:	1.42776	8:	120.12592
	9-10:	1.42792	9:	119.79982
	10-7:	1.42951	10:	119.99319
	7-3:	1.43350	7:	120.47163
2	4-5:	1.42848	5/19:	118.34876
	5-16:	1.42012	16/20:	122.22626
	16-15:	1.37554	15/21:	120.63833
	15-14:	1.42331	14/22:	118.78421
	14-8:	1.42762	8/10:	120.24908
	8-4:	1.43021	4/7:	119.75197
3	8-14:	1.42762	8:	119.62180
	14-13:	1.41646	14:	118.55365
	13-12:	1.37769	13:	122.19203
	12-11:	1.42084	12:	120.49128
	11-9:	1.42846	11:	118.87392
	9-8:	1.42776	9:	120.26564

Member Ring	Bond length (angstrom)		Atom internal angle (degree)	
4	10-9:	1.42792	10:	119.98213
	9-11:	1.42846	9:	119.93392
	11-23:	1.41787	11:	118.42074
	23-24:	1.37622	23:	122.11916
	24-22:	1.42307	24:	120.61106
	22-10:	1.42890	22:	118.93075
5	19-7:	1.42614	19:	119.00075
	7-10:	1.42951	7:	119.80004
	10-22:	1.42890	10:	120.02368
	22-21:	1.41623	22:	118.38679
	21-20:	1.37643	21:	121.94984
	20-19:	1.42010	20:	120.81048
6	17-2:	1.43036	17:	120.16520
	2-3:	1.43288	2:	118.12740
	3-7:	1.43350	3:	120.79674
	7-19:	1.42614	7:	119.72667
	19-18:	1.41692	19:	117.86864
	18-17:	1.37807	18:	123.21434
7	1-6:	1.38692	1:	120.76956
	6-5:	1.41644	6:	121.58222
	5-4:	1.42848	5:	118.91585
	4-3:	1.42882	4:	119.82967
	3-2:	1.43288	3:	120.01045
	2-1:	1.42165	2:	118.88923

50

Member Ring	Bond length (angstrom)		Atom internal angle (degree)	
4	10-9:	1.42293	10:	120.02946
	9-11:	1.43064	9:	119.96912
	11-23:	1.42332	11:	119.93908
	23-24:	1.42858	23:	120.16171
	24-22:	1.42437	24:	119.89291
	22-10:	1.43071	22:	120.00473
5	19-7:	1.43068	19:	120.01237
	7-10:	1.42293	7:	120.01618
	10-22:	1.43071	10:	119.97503
	22-21:	1.42325	22:	119.94373
	21-20:	1.42857	21:	120.15194
	20-19:	1.42437	20:	119.89745
6	17-2:	1.42434	17:	119.91325
	2-3:	1.43064	2:	119.99631
	3-7:	1.42297	3:	120.02053
	7-19:	1.43068	7:	119.98470
	19-18:	1.42325	19:	119.93211
	18-17:	1.42861	18:	120.15017
7	1-6:	1.42857	1:	120.16126
	6-5:	1.42436	6:	119.89392
	5-4:	1.43071	5:	120.00362
	4-3:	1.42293	4:	120.02955
	3-2:	1.43064	3:	119.96938
	2-1:	1.42331	2:	119.93875
8	35-38:	1.40530	35:	119.41607
	38-37:	1.40595	38:	121.67373
	37-16:	1.43419	37:	119.38318
	16-5:	1.42327	16:	119.76385
	5-6:	1.42436	5:	120.05007
	6-35:	1.43438	6:	119.71119
9	16-37:	1.43419	16:	120.08498
	37-39:	1.42726	37:	117.79116
	39-41:	1.36788	39:	122.66128
	41-40:	1.43449	41:	120.80446
	40-15:	1.43435	40:	118.27809
	15-16:	1.42858	15:	120.37930
10	14-15:	1.42438	14:	120.05458
	15-40:	1.43435	15:	119.72193
	40-42:	1.40535	40:	119.40122
	42-43:	1.40600	42:	121.67916
	43-13:	1.43419	43:	119.38907
	13-14:	1.42324	13:	119.75305



Member Ring	Bond length (angstrom)		Atom internal angle (degree)	
11	12-13:	1.42861	12:	120.38656
	13-43:	1.43419	13:	120.09500
	43-44:	1.42741	43:	117.77106
	44-46:	1.36788	44:	122.66022
	46-45:	1.43432	46:	120.82309
	45-12:	1.43428	45:	118.26306
12	23-11:	1.42332	23:	119.76006
	11-12:	1.42433	11:	120.06354
	12-45:	1.43428	12:	119.69936
	45-47:	1.40530	45:	119.42112
	47-48:	1.40599	47:	121.68207
	48-23:	1.43419	48:	119.37229
13	50-24:	1.43440	50:	118.26697
	24-23:	1.42858	24:	120.39436
	23-48:	1.43419	23:	120.07759
	48-49:	1.42736	48:	117.78948
	49-51:	1.36791	49:	122.66283
	51-50:	1.43446	51:	120.80811
14	52-21:	1.43418	52:	119.38584
	21-22:	1.42325	21:	119.76285
	22-24:	1.42437	22:	120.05014
	24-50:	1.43440	24:	119.71222
	50-53:	1.40533	50:	119.41379
	53-52:	1.40591	53:	121.67399
15	32-31:	1.43449	32:	120.80410
	31-20:	1.43435	31:	118.27788
	20-21:	1.42857	20:	120.37897
	21-52:	1.43418	21:	120.08420
	52-54:	1.42723	52:	117.79313
	54-32:	1.36789	54:	122.66059
16	29-28:	1.40603	29:	121.67860
	28-18:	1.43420	28:	119.38833
	18-19:	1.42325	18:	119.75348
	19-20:	1.42437	19:	120.05411
	20-31:	1.43435	20:	119.72258
	31-29:	1.40534	31:	119.40135
17	30-26:	1.36787	30:	122.66086
	26-25:	1.43432	26:	120.82360
	25-17:	1.43428	25:	118.26276
	17-18:	1.42861	17:	120.38673
	18-28:	1.43420	18:	120.09584
	28-30:	1.42742	28:	117.76945

Member Ring	Bond length (angstrom)		Atom internal angle (degree)	
18	25-27:	1.40531	25:	119.42124
	27-33:	1.40598	27:	121.68209
	33-1:	1.43419	33:	119.37228
	1-2:	1.42331	1:	119.76024
	2-17:	1.42434	2:	120.06364
	17-25:	1.43428	17:	119.69930
19	33-34:	1.42736	33:	117.78956
	34-36:	1.36791	34:	122.66202
	36-35:	1.43444	36:	120.80815
	35-6:	1.43438	35:	118.26827
	6-1:	1.42857	6:	120.39335
	1-33:	1.43419	1:	120.07722

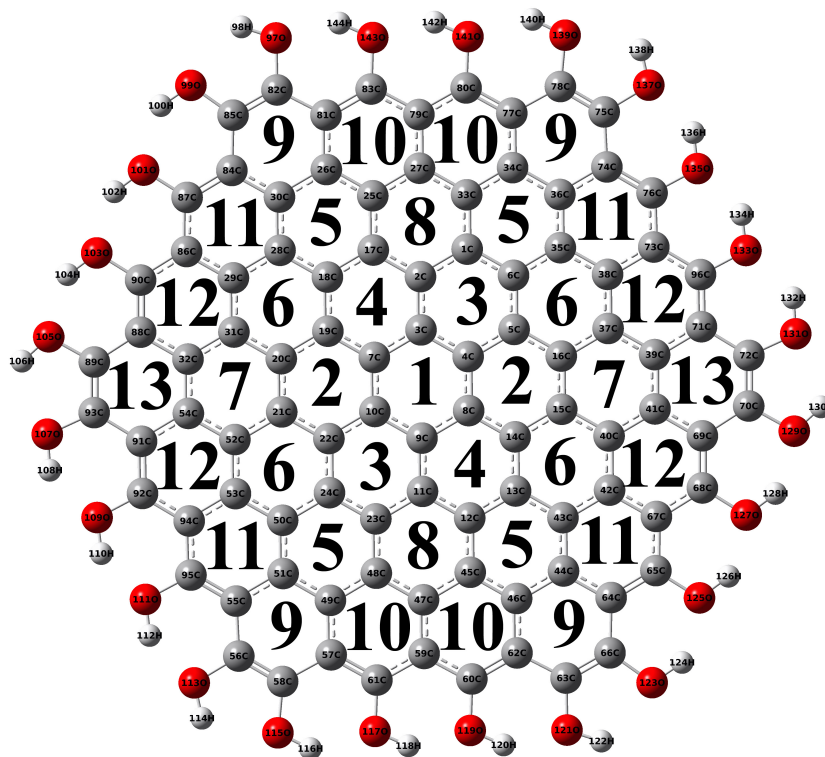


***Figure 4.11 Structure of  $C_{96}$  graphene nano disk with OH-dopants***

Member Ring	Bond length (angstrom)		Atom Internal angle (degree)	
1	3-4:	1.42291	3:	119.99975
	4-8:	1.42290	4:	119.99994
	8-9:	1.42290	8:	120.00002
	9-10:	1.42290	9:	119.99965
	10-7:	1.42291	10:	120.00004
	7-3:	1.42290	7:	119.99993
2	5-16:	1.42363	5:	119.95149
	16-15:	1.39837	16:	120.01024
	15-14:	1.42338	15:	120.10989
	14-8:	1.40156	14:	119.92792
	8-4:	1.42290	8:	119.98255
	4-5:	1.42290	4:	120.01740
3	8-14:	1.40156	8:	120.01716
	14-13:	1.42363	14:	119.95173
	13-12:	1.39837	13:	120.01011
	12-11:	1.42339	12:	120.10971
	11-9:	1.40156	11:	119.92836
	9-8:	1.42290	9:	119.98242

Member Ring	Bond length (angstrom)		Atom Internal angle (degree)	
4	10-9:	1.42290	10:	119.98227
	9-11:	1.40156	9:	120.01761
	11-23:	1.42363	11:	119.95144
	23-24:	1.39838	23:	120.00967
	24-22:	1.42338	24:	120.11005
	22-10:	1.40156	22:	119.92833
5	19-7:	1.40156	19:	119.92823
	7-10:	1.42291	7:	119.98256
	10-22:	1.40156	10:	120.01738
	22-21:	1.42363	22:	119.95132
	21-20:	1.39838	21:	120.01051
	20-19:	1.42339	20:	120.10946
6	17-2:	1.42338	17:	120.10964
	2-3:	1.40156	2:	119.92843
	3-7:	1.42290	3:	119.98247
	7-19:	1.40156	7:	120.01723
	19-18:	1.42362	19:	119.95180
	18-17:	1.39839	18:	120.00994
7	1-6:	1.39839	1:	120.00942
	6-5:	1.42339	6:	120.11020
	5-4:	1.42290	5:	119.92816
	4-3:	1.42291	4:	119.98237
	3-2:	1.40156	3:	120.01752
	2-1:	1.42363	2:	119.95171
8	35-38:	1.42455	35:	119.98173
	38-37:	1.42307	38:	120.06656
	37-16:	1.42910	37:	119.95701
	16-5:	1.42363	16:	119.95189
	5-6:	1.42339	5:	120.12009
	6-35:	1.42859	6:	119.92229
9	16-37:	1.42910	16:	120.03766
	37-39:	1.42859	37:	120.07421
	39-41:	1.42780	39:	119.78612
	41-40:	1.40051	41:	120.13605
	40-15:	1.42860	40:	119.99810
	15-16:	1.39837	15:	119.96761
10	14-15:	1.42338	14:	120.12016
	15-40:	1.42860	15:	119.92234
	40-42:	1.42453	40:	119.98128
	42-43:	1.42309	42:	120.06763
	43-13:	1.42910	43:	119.95596
	13-14:	1.42363	13:	119.95231

Member Ring	Bond length (angstrom)		Atom Internal angle (degree)	
11	12-13:	1.39837	12:	119.96741
	13-43:	1.42910	13:	120.03741
	43-44:	1.40189	43:	120.07476
	44-46:	1.42780	44:	119.78672
	46-45:	1.40052	46:	120.13422
	45-12:	1.42860	45:	119.99924
12	23-11:	1.42363	23:	119.95235
	11-12:	1.42339	11:	120.11994
	12-45:	1.42860	12:	119.92271
	45-47:	1.42452	45:	119.98018
	47-48:	1.42308	47:	120.06905
	48-23:	1.42909	48:	119.95528
13	50-24:	1.42859	50:	119.99921
	24-23:	1.39838	24:	119.96652
	23-48:	1.42909	23:	120.03771
	48-49:	1.40190	48:	120.07517
	49-51:	1.42779	49:	119.78464
	51-50:	1.40051	51:	120.13624
14	52-21:	1.42909	52:	119.95673
	21-22:	1.42363	21:	119.95136
	22-24:	1.42338	22:	120.12010
	24-50:	1.42859	24:	119.92316
	50-53:	1.42453	50:	119.98007
	53-52:	1.42307	53:	120.06819
15	32-31:	1.40050	32:	120.13894
	31-20:	1.42860	31:	119.99653
	20-21:	1.39838	20:	119.96741
	21-52:	1.42909	21:	120.03794
	52-54:	1.40189	52:	120.07475
	54-32:	1.42778	54:	119.78411
16	29-28:	1.42309	29:	120.06386
	28-18:	1.42911	28:	119.95881
	18-19:	1.42362	18:	119.95170
	19-20:	1.42339	19:	120.11977
	20-31:	1.42860	20:	119.92294
	31-29:	1.42455	31:	119.98257
17	30-26:	1.42779	30:	119.78765
	26-25:	1.40050	26:	120.13709
	25-17:	1.42861	25:	119.99635
	17-18:	1.39839	17:	119.96796
	18-28:	1.42911	18:	120.03821
	28-30:	1.40187	28:	120.07244

Member Ring	Bond length (angstrom)		Atom Internal angle (degree)	
18	25-27:	1.42454	25:	119.98328
	27-33:	1.42310	27:	120.06420
	33-1:	1.42910	33:	119.95795
	1-2:	1.42363	1:	119.95218
	2-17:	1.42338	2:	120.11962
	17-25:	1.42861	17:	119.92225
19	33-34:	1.40188	33:	120.07249
	34-36:	1.42778	34:	119.78750
	36-35:	1.40049	36:	120.13641
	35-6:	1.42859	35:	119.99767
	6-1:	1.39839	6:	119.96723
	1-33:	1.42910	1:	120.03814
20	36-74:	1.43201	36:	119.82461
	74-76:	1.36989	74:	119.66081
	76-73:	1.42254	76:	121.82277
	73-38:	1.41172	73:	118.77693
	38-35:	1.42455	38:	119.89425
	35-36:	1.40049	35:	120.02042
21	38-73:	1.41172	38:	120.03906
	73-96:	1.42415	73:	118.80119
	96-71:	1.37165	96:	121.61722
	71-39:	1.43232	71:	119.79191
	39-37:	1.42859	39:	119.78179
	37-38:	1.42307	37:	119.96863
22	39-71:	1.43232	39:	120.43203
	71-72:	1.45609	71:	117.95319
	72-70:	1.33071	72:	121.06211
	70-59:	1.44809	70:	122.96513
	59-41:	1.43199	59:	117.54845
	41-39:	1.42780	41:	120.03904
23	40-41:	1.40051	40:	120.02055
	41-69:	1.43199	41:	119.82485
	69-68:	1.36992	69:	119.66014
	68-67:	1.42251	68:	121.82217
	67-42:	1.41172	67:	118.77811
	42-40:	1.42453	42:	119.89396
24	43-42:	1.42309	43:	120.02055
	42-57:	1.41172	42:	119.96917
	57-65:	1.42416	57:	120.03834
	65-64:	1.37163	65:	121.61762
	64-44:	1.43233	64:	119.79202
	44-43:	1.40189	44:	119.78131

Member Ring	Bond length (angstrom)		Atom Internal angle (degree)	
25	46-44:	1.42780	46:	120.04049
	44-64:	1.43233	44:	120.43190
	64-66:	1.45609	64:	117.95242
	66-63:	1.33069	66:	121.06304
	63-62:	1.44812	63:	122.96655
	62-46:	1.43201	62:	117.54554
26	47-45:	1.42452	47:	119.89383
	45-46:	1.40052	45:	120.02044
	46-62:	1.43201	46:	119.82521
	62-60:	1.36994	62:	119.65829
	60-59:	1.42249	60:	121.82211
	59-47:	1.41170	59:	118.78004
27	49-48:	1.40190	49:	119.78208
	48-47:	1.42308	48:	119.96935
	47-59:	1.41170	47:	120.03701
	59-61:	1.42414	59:	118.80369
	61-57:	1.37165	61:	121.61778
	57-49:	1.43234	57:	119.78942
28	55-51:	1.43201	55:	117.54732
	51-49:	1.42779	51:	120.03924
	49-57:	1.43234	49:	120.43309
	57-58:	1.45611	57:	117.95085
	58-56:	1.33070	58:	121.06280
	56-55:	1.44808	56:	122.96644
29	94-53:	1.41170	94:	118.77955
	53-50:	1.42453	53:	119.89359
	50-51:	1.40051	50:	120.02050
	51-55:	1.43201	51:	119.82425
	55-95:	1.36991	55:	119.65974
	95-94:	1.42250	95:	121.82215
30	91-54:	1.43235	91:	119.78972
	54-52:	1.40189	54:	119.78285
	52-53:	1.42307	52:	119.96838
	53-94:	1.41170	53:	120.03806
	94-92:	1.42414	94:	118.80351
	92-91:	1.37164	92:	121.61732
31	89-88:	1.44807	89:	122.96509
	88-32:	1.43197	88:	117.55101
	32-54:	1.42778	32:	120.03790
	54-91:	1.43235	54:	120.43288
	91-93:	1.45612	91:	117.95173
	93-89:	1.33071	93:	121.06109

Member Ring	Bond length (angstrom)		Atom Internal angle (degree)	
32	90-86:	1.42257	90:	121.82346
	86-29:	1.41176	86:	118.77245
	29-31:	1.42455	29:	119.89575
	31-32:	1.40050	31:	120.02079
	32-88:	1.43197	32:	119.82313
	88-90:	1.36986	88:	119.66409
33	87-84:	1.37161	87:	121.61704
	84-30:	1.43231	84:	119.79523
	30-28:	1.40187	30:	119.78116
	28-29:	1.42309	28:	119.96865
	29-86:	1.41176	29:	120.04031
	86-87:	1.42420	86:	118.79754
34	85-82:	1.33069	85:	121.06203
	82-81:	1.44809	82:	122.96439
	81-26:	1.43197	81:	117.54934
	26-30:	1.42779	26:	120.03883
	30-84:	1.43231	30:	120.43106
	84-85:	1.45607	84:	117.95419
35	81-83:	1.36990	81:	119.66299
	83-79:	1.42255	83:	121.82295
	79-27:	1.41176	79:	118.77326
	27-25:	1.42454	27:	119.89640
	25-26:	1.40050	25:	120.02021
	26-81:	1.43197	26:	119.82402
36	79-80:	1.42421	79:	118.79775
	80-77:	1.37161	80:	121.61745
	77-34:	1.43232	77:	119.79501
	34-33:	1.40188	34:	119.78046
	33-27:	1.42310	33:	119.96935
	27-79:	1.41176	27:	120.03930
37	77-78:	1.45608	77:	117.95356
	78-75:	1.33069	78:	21.06255
	75-74:	1.44809	75:	122.96497
	74-36:	1.43201	74:	117.54791
	36-34:	1.42778	36:	120.03868
	34-77:	1.43232	34:	120.43188



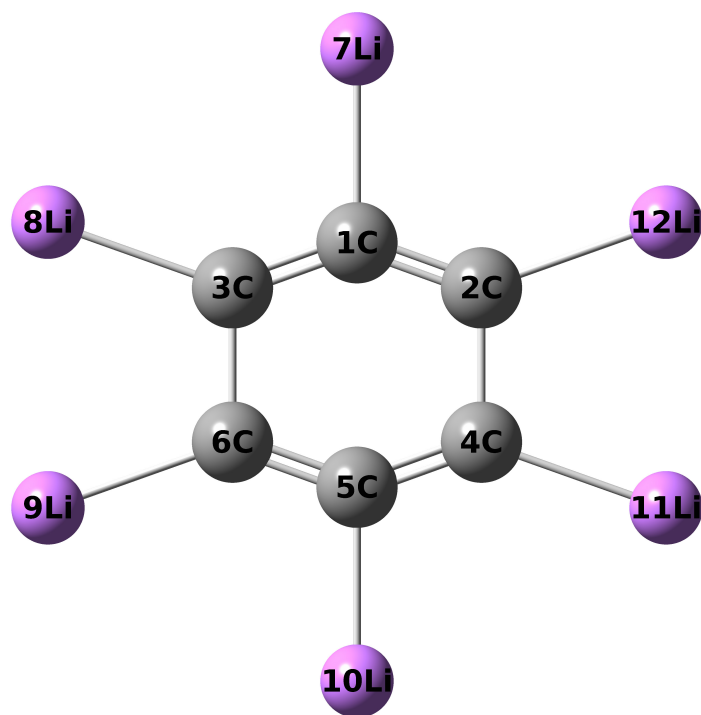


***Figure 4.12 Structure of  $C_6$  graphene nano disk with Li-dopants***

Bond length (angstrom)		Atom internal angle (degree)	
1-2:	1.3529665	1:	140.2282938
2-4:	1.5754580	2:	109.8858531
4-5:	1.3529665	4:	109.8858531
5-6:	1.3529665	5:	140.2282938
6-3:	1.5754580	6:	109.8858531
3-1:	1.3529665	3:	109.8858531

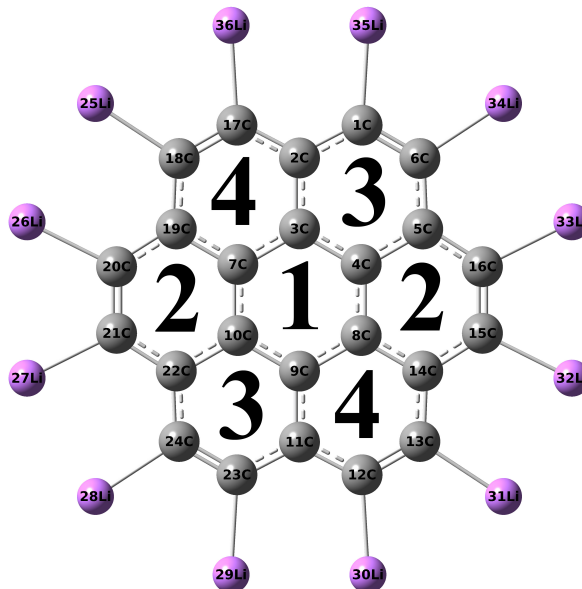


***Figure 4.13 Structure of  $C_{24}$  graphene nano disk with Li-dopants***

Member Ring	Bond length (angstrom)	Atom internal angle (degree)
1	3-4:	1.44599
	3:	120.00003
	4-8:	1.44599
	4:	119.99999
	8-9:	1.44599
	8:	119.99999
2	9-10:	1.44599
	9:	120.00003
	10-7:	1.44599
	10:	119.99999
	7-3:	1.44599
	7:	119.99999
3	4-5/7-19:	1.44258
	5/19:	117.66782
	5-16/19-20:	1.43419
	16/20:	122.33215
	16-15/20-21:	1.35448
	15/21:	122.33215
4	15-14/21-22:	1.43419
	14/22:	117.66782
	14-8/22-10:	1.44258
	8/10:	120.00002
	8-4/10-7:	1.44599
	4/7:	120.00002
5	2-1/11-23:	1.43419
	1/23:	122.33217
	1-6/23-24:	1.35448
	6/24:	122.33217
	6-5/24-22:	1.43419
	5/22:	117.66787
6	5-4/22-10:	1.44258
	4/10:	119.99999
	4-3/10-9:	1.44599
	3/9:	119.99999
	3-2/9-11:	1.44258
	2/11:	117.66782
7	18-17/13-12:	1.35448
	17/12:	122.33217
	17-2/12-11:	1.43419
	2/11:	117.66782
	2-3/11-9:	1.44258
	3/9:	119.99999
8	3-7/9-8:	1.44599
	7/8:	119.99999
	7-19/8-14:	1.44258
9	19/14:	117.66787
	19-18/14-13:	1.43419
10	18/13:	122.33217

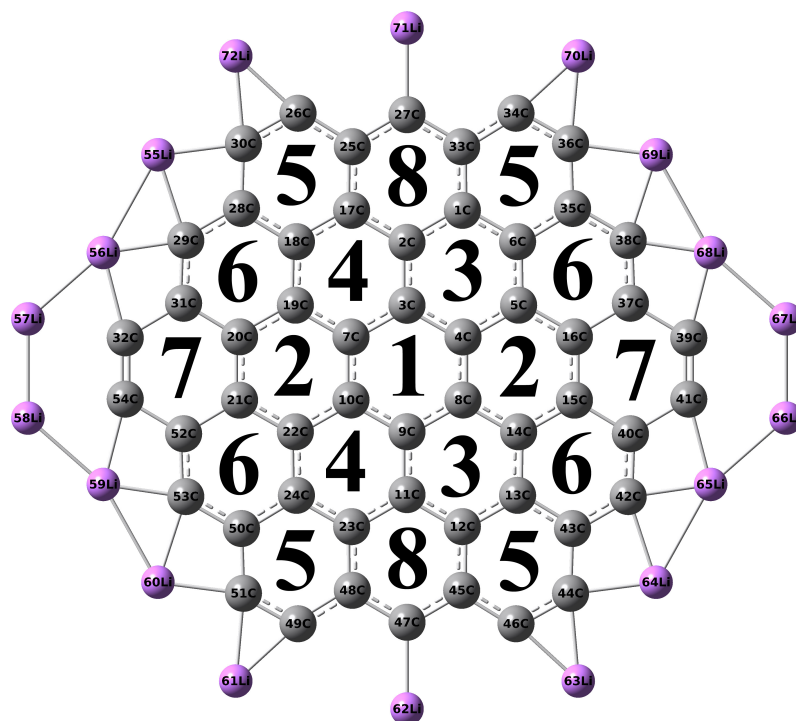


***Figure 4.14 Structure of  $C_{54}$  graphene nano disk with Li-dopants***

Member Ring	Bond length (angstrom)		Atom internal angle (degree)	
1	3-4:	1.44075	3:	120.90137
	4-8:	1.41396	4:	119.54931
	8-9:	1.44075	8:	119.54931
	9-10:	1.44075	9:	120.90137
	10-7:	1.41396	10:	119.54931
	7-3:	1.44075	7:	119.54931
	4-5/7-19:	1.43452	5/19:	120.58743
2	5-16/19-20:	1.43651	16/20:	119.62185
	16-15/20-21:	1.41933	15/21:	119.62185
	15-14/21-22:	1.43651	14/22:	120.58743
	14-8/22-10:	1.43452	8/10:	119.79072
	8-4/10-7:	1.41396	4/7:	119.79072
	2-1/11-23:	1.43209	1/23:	120.32402
	1-6/23-24:	1.42080	6/24:	120.55583
3	6-5/24-22:	1.42501	5/22:	118.84018
	5-4/22-10:	1.43452	4/10:	120.65997
	4-3/10-9:	1.44075	3/9:	119.54931
	3-2/9-11:	1.41133	2/11:	120.07069

Member Ring	Bond length (angstrom)	Atom internal angle (degree)
4	18-17/13-12:	1.42080 17/12: 120.32402
	17-2/12-11:	1.43209 2/11: 120.07069
	2-3/11-9:	1.41133 3/9: 119.54931
	3-7/9-8:	1.44075 7/8: 120.65997
	7-19/8-14:	1.43452 19/14: 118.84018
	19-18/14-13:	1.42501 18/13: 120.55583
5	25-26/33-34/43-44/48-49:	1.42874 26/34/46/49: 119.12366
	26-30/34-36/44-46/49-51:	1.39901 30/36/44/51: 120.94694
	30-28/36-35/46-45/51-50:	1.45398 28/35/43/50: 119.42787
	28-18/35-6/45-12/50-24:	1.43746 18/6/13/24: 119.22243
	18-17/6-1/12-13/24-23:	1.42080 17/1/12/23: 120.25377
	17-25/1-33/13-43/23-48:	1.42791 25/33/45/48: 121.02534
6	18-28/6-35/24-50/13-43:	1.43746 28/35/50/43: 118.90274
	28-29/35-38/50-53/43-42:	1.43746 29/38/53/42: 121.93409
	29-31/38-37/53-52/42-40:	1.40916 31/37/52/40: 119.01753
	31-20/37-16/52-21/40-15:	1.46188 20/16/21/15: 119.35150
	20-19/16-5/21-22/15-14:	1.43651 19/5/22/14: 120.57240
	19-18/5-6/22-24/14-13:	1.42501 18/6/24/13: 120.22175
7	16-37/20-31:	1.46188 37/31: 118.24698
	37-39/31-32:	1.51951 39/32: 120.72638
	39-41/32-54:	1.37359 41/54: 120.72638
	41-40/54-52:	1.51951 40/52: 118.24698
	40-15/52-21:	1.46188 15/21: 121.02664
	15-16/21-20:	1.41933 16/20: 121.02664
8	25-27/48-47:	1.41786 27/47: 119.24094
	27-33/47-45:	1.41786 33/45: 121.02801
	33-1/45-12:	1.42791 1/12: 119.42221
	1-2/12-11:	1.43209 2/11: 119.85861
	2-17/11-23:	1.43209 17/23: 119.42221
	17-25/23-48:	1.42791 25/48: 121.02801

## 4.2 Stability of graphene nano disks with edge-dopants

We examined the effect of edge-doping on stability by calculating the stabilization energies of graphene nano disks with the following equation:

$$E_{st} = \frac{E_{Doped-graphene} - n \times E_C - m \times E_{dopant}}{n} \quad (7)$$

where  $E_{st}$ ,  $E_{Doped-graphene}$ ,  $E_C$ , and  $E_{dopant}$  are stabilization energy of graphene, system energy of graphene, energy of a carbon atom, and energy of dopant, which were obtained from B3lyp calculations. The  $n$  and  $m$  are numbers of carbon atoms and dopants contained in a graphene, respectively. As shown in Figure 4.15, doping H, Li, F or OH to the edge of GNDs increases the stabilization energies. Furthermore, for Li-doped GNDs, the stabilization energy increases with increasing number of carbon atoms. In contrast, the stabilization energy decreases with increasing number of carbon atoms in H-, F- or OH- doped GNDs. This indicates that the doping effect on the stability of graphene nano disk is dependent on the type of dopants.

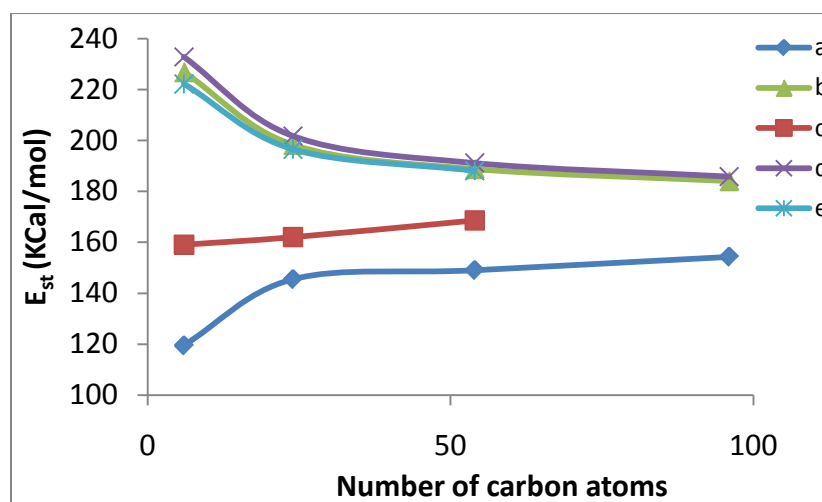


**Figure 4.15 Stabilization energy ( $E_{st}$ ) of graphene vs. its number of carbon atoms: (a) without edge-doping, (b) H-doped, (c) Li-doped, (d) F-doped, and (e) OH-doped.**

### ***4.3 HOMO-LUMO energy gaps of graphene nano disks with edge-dopants***

HOMO-LUMO energy gaps of graphene nano disks with edge-dopants were calculated by using Pw91pw91/6-31g(d) method based on the geometries optimized via B3lyp/6-31g(d) calculations. From Figure 4.16, one can see that the HOMO-LUMO energy gap of the graphene nano disk increases if its edge is doped with H, F, or OH. As a result, H, F, or OH-doped C6 GND is insulator with a HOMO-LUMO gap above 4 eV. However, H, F, or OH-doped C24, C54, and C96 GNDs are semi-conductors, because their HOMO-LUMO gaps are in the range of 1 to 3eV. Different from the H, F, and OH-doping, doping a GND with Li could decrease its HOMO-LUMO gap. As a result, its HOMO-LUMO energy gap is below 0.2 eV. Therefore, Li-doped GNDs are organic metals.

The dependence of HOMO-LUMO band gap on properties of dopants was also observed in the case of graphene nanoribbon (GNR) (63-65). For example, N and B can produce different effects on the band gap of GNR (63). Furthermore, it was reported that GNR with edge doping of N atoms exhibited typical n-type behavior while B-doped GNR showed p-type behavior (64, 65). Compared with the GNR, GNDs are more sensitive to edge-dopants, namely, edge-doping can transfer a GND from its semiconductor state into a conductor state.

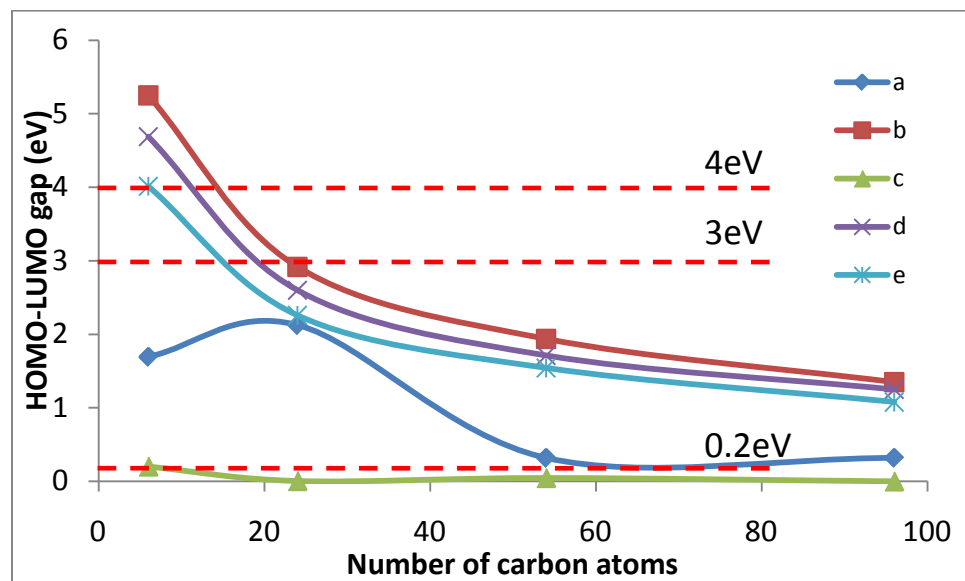


**Figure 4.16 HOMO-LUMO energy gap of graphene nano disks: (a) without doping, (b) H-doped, (c) Li-doped, (d) F-doped, and (e) OH-doped.**

## Chapter 5

### Conclusions

The B3lyp and Pw91pw91 DFT calculations were employed to evaluate the structures and properties of graphene nano disks (GND) with a concentric shape in this research. From the research, we can make the following conclusions:

- (1). There are two types of edges—Zigzag and Armchair in concentric graphene nano disks (GND). The bond length between armchair-edge carbons is much shorter than that between zigzag-edge carbons. For C24 GND that consists of 24 carbon atoms, only armchair edge with 12 atoms is formed. For a concentric GND larger than the C24 GND, both armchair and zigzag edges co-exist. Furthermore, although the number of armchair-edge carbon atoms is always 12, the number of zigzag-edge atoms increases with increasing the size of the GND.
- (2). The stability of a GND increases with increasing its size.
- (3). The HOMO-LUMO energy gap of a graphene nano disk is dependent on its size. The C6 and C24 GNDs possess HOMO-LUMO gaps of 1.7 and 2.1eV, respectively, indicating that they are semi-conductors. However, C54 and C96 GNDs are organic metals, because their HOMO-LUMO gaps are as low as 0.3eV.
- (4). Doping the edge of a graphene nano disk can change its structure, stability, and HOMO-LUMO energy gaps. When doped foreign atoms are attached to the edge of a GND, the original unsaturated carbon atoms become saturated. As a result, its bond lengths between carbon atoms and its stability increase. Furthermore, the doping effect on the HOMO-LUMO energy gap is dependent on type of doped



atoms. When H, F, and OH are used as dopants for a GND, its HOMO-LUMO energy gap are increases. In contrast, Li-doping decreases the HOMO-LUMO energy gap of a graphene nano disk. Therefore, Li-doping can increase the electrical conductance of a GND, whereas H, F, or OH-doping should decrease its conductance.

## References

- (1). Kroto HW, Heath JR, O'Brien SC, Curl RF, Smalley RE. C-60 Buckminsterfullerene. *Nature*. 1985;318(6042):162-163.
- (2). Iijima S. Helical Microtubules of Graphitic Carbon. *Nature*. 1991;354(6348):56-58.
- (3). Boehm HP, Setton R, Stumpp E. Nomenclature and Terminology of Graphite-Intercalation Compounds (Iupac Recommendations 1994). *Pure and Applied Chemistry*. 1994;66(9):1893-1901.
- (4). Peierls RE. Quelques proprietes typiques des corps solides. *Annales de l'Institut Henri Poincaré*. 1935;5:177-222.
- (5). Landau LD. Zur Theorie der phasenumwandlungen II. *Physik Zeitschrift Sowjetunion*. 1937;11:26-35.
- (6). Shioyama H. Cleavage of graphite to graphene. *Journal of Materials Science Letters*. 2001;20(6):499-500.
- (7). Novoselov KS, Geim AK, Morozov SV, Jiang D, Zhang Y, Dubonos SV, Grigorieva IV, Firsov AA. Electric field effect in atomically thin carbon films. *Science*. 2004;306(5696):666-669.
- (8). Novoselov KS, Geim AK, Morozov SV, Jiang D, Katsnelson MI, Grigorieva IV, Dubonos SV, Firsov AA. Two-dimensional gas of massless Dirac fermions in graphene. *Nature*. 2005;438(7065):197-200.
- (9). Zhang YB, Tan YW, Stormer HL, Kim P. Experimental observation of the quantum Hall effect and Berrys phase in graphene. *Nature*. 2005;438(7065):201-204.
- (10). Berger C, Song ZM, Li XB, Wu XS, Brown N, Naud C, Mayou D, Li TB, Hass J, Marchenkov AN and others. Electronic confinement and coherence in patterned epitaxial graphene. *Science*. 2006;312(5777):1191-1196.
- (11). Meyer JC, Geim AK, Katsnelson MI, Novoselov KS, Booth TJ, Roth S. The structure of suspended graphene sheets. *Nature*. 2007;446(7131):60-63.
- (12). Hernandez Y, Nicolosi V, Lotya M, Blighe FM, Sun ZY, De S, McGovern IT, Holland B, Byrne M, Gunko YK and others. High-yield production of graphene by liquid-phase exfoliation of graphite. *Nature Nanotechnology*. 2008;3(9):563-568.

- (13) Geim AK, Novoselov KS. The rise of graphene. *Nature Materials*. 2007;6(3):183-191.
- (14) Geim AK, MacDonald AH. Graphene: Exploring carbon flatland. *Physics Today*. 2007;60(8):35-41.
- (15) Katsnelson MI. Graphene: carbon in two dimensions. *Materials Today*. 2007;10(1-2):20-27.
- (16) Neto AC, Guinea F, Peres NMR. Drawing conclusions from graphene. *Physics World*. 2006;19(11):33-37.
- (17) Schedin F, Geim AK, Morozov SV, Hill EW, Blake P, Katsnelson MI, Novoselov KS. Detection of individual gas molecules adsorbed on graphene. *Nature Materials*. 2007;6(9):652-655.
- (18) Dikin DA, Stankovich S, Zimney EJ, Piner RD, Dommett GHB, Evmenenko G, Nguyen ST, Ruoff RS. Preparation and characterization of graphene oxide paper. *Nature*. 2007;448(7152):457-460.
- (19) Elias DC, Nair RR, Mohiuddin TMG, Morozov SV, Blake P, Halsall MP, Ferrari AC, Boukhvalov DW, Katsnelson MI, Geim AK and others. Control of Graphene's Properties by Reversible Hydrogenation: Evidence for Graphane. *Science*. 2009;323(5914):610-613.
- (20) Geim AK. Graphene: Status and Prospects. *Science*. 2009;324(5934):1530-1534.
- (21) Sutter P. EPITAXIAL GRAPHENE How silicon leaves the scene. *Nature Materials*. 2009;8(3):171-172.
- (22) Coey JMD, Venkatesan M, Fitzgerald CB, Douvalis AP, Sanders IS. Ferromagnetism of a graphite nodule from the Canyon Diablo meteorite. *Nature*. 2002;420:156-159.
- (23) Berger C, Song ZM, Li TB, Li XB, Ogbazghi AY, Feng R, Dai ZT, Marchenkov AN, Conrad EH, First PN and others. Ultrathin epitaxial graphite: 2D electron gas properties and a route toward graphene-based nanoelectronics. *Journal of Physical Chemistry B*. 2004;108:19912-19916.
- (24) Rollings E, Gweon GH, Zhou SY, Mun BS, McChesney JL, Hussain BS, Fedorov A, First PN, de Heer WA, Lanzara A. Synthesis and characterization of atomically thin graphite films on a silicon carbide substrate. *Journal of Physics and Chemistry of Solids*. 2006;67(9-10):2172-2177.
- (25) Tung VC, Allen MJ, Yang Y, Kaner RB. High-throughput solution processing of large-scale graphene. *Nature Nanotechnology*. 2009;4(1):25-29.

- (26) Dreyer DR, Park S, Bielawski CW, Ruoff RS. The chemistry of graphene oxide. *Chemical Society Reviews*. 2010;39(1):228-240.
- (27) Brodie BC. On the atomic weight of graphite. *Philosophical Transactions of the Royal Society of London*. 1859;149:249-259.
- (28) Hummers WS, Offeman RE. Preparation of Graphitic Oxide. *Journal of the American Chemical Society*. 1958;80(6):1339-1339.
- (29) Hu YH, Wang H, Hu B. Thinnest Two-Dimensional Nanomaterial-Graphene for Solar Energy. *Chemsuschem*. 2010;3(7):782-796.
- (30) Wallace PR. The Band Theory of Graphite. *Physical Review Online Archive (Prola)*. 1947;71(9):622-634.
- (31) Castro Neto AH, Guinea F, Peres NMR, Novoselov KS, Geim AK. The electronic properties of graphene. *Reviews of Modern Physics*. 2009;81(1):109-162.
- (32) Zheng YS, Ando T. Hall conductivity of a two-dimensional graphite system. *Physical Review B*. 2002;65(24):245420.
- (33) Akturk A, Goldsman N. Electron transport and full-band electron-phonon interactions in graphene. *Journal of Applied Physics*. 2008;103(5):053702.
- (34) Li YF, Zhou Z, Yu GT, Chen W, Chen ZF. CO Catalytic Oxidation on Iron-Embedded Graphene: Computational Quest for Low-Cost Nanocatalysts. *Journal of Physical Chemistry C*. 2010;114(14):6250-6254.
- (35) Åhlgren EH, Kotakoski J, Krasheninnikov AV. Atomistic simulations of the implantation of low-energy boron and nitrogen ions into graphene. *Physical Review B*. 2011;83(11):115424.
- (36) Ao ZM, Jiang Q, Zhang RQ, Tan TT, Li S. Al doped graphene: A promising material for hydrogen storage at room temperature. *Journal of Applied Physics*. 2009;105(7):074307.
- (37) Nakada K, Fujita M, Dresselhaus G, Dresselhaus MS. Edge state in graphene ribbons: Nanometer size effect and edge shape dependence. *Physical Review B*. 1996;54(24):17954-17961.
- (38) Zhao P, Choudhury M, Mohanram K, Guo J. Computational Model of Edge Effects in Graphene Nanoribbon Transistors. *Nano Research*. 2008;1(5):395-402.

- (39) Sako R, Hosokawa H, Tsuchiya H. Computational Study of Edge Configuration and Quantum Confinement Effects on Graphene Nanoribbon Transport. *IEEE Electron Device Letters*. 2011;6-8.
- (40) Oeiras RY, Araujo-Moreira FM, da Silva EZ. Defect-mediated half-metal behavior in zigzag graphene nanoribbons. *Physical Review B*. 2009;80(7):073405.
- (41) Cervantes-Sodi F, Csanyi G, Piscanec S, Ferrari AC. Edge-functionalized and substitutionally doped graphene nanoribbons: Electronic and spin properties. *Physical Review B*. 2008;77(16):165427.
- (42) Yijian O, Youngki Y, Jing G. Edge chemistry engineering of graphene nanoribbon transistors: A computational study. *IEDM 2008. IEEE International Electron Devices Meeting. Technical Digest*. 2008:4.
- (43) Berashevich J, Chakraborty T. Doping graphene by adsorption of polar molecules at the oxidized zigzag edges. *Physical Review B*. 2010;81(20):205431.
- (44) Cocchi C, Ruini A, Prezzi D, Cadas MJ, Molinari E. Designing All-Graphene Nanojunctions by Covalent Functionalization. *Journal of Physical Chemistry C*. 2011;115(7):2969-2973.
- (45) Hehre WJ, Pople JA, Radom L, Schleyer PR. *An initio Molecular Orbital Theory*, A Wiley-International Publication, 1986
- (46) Hartree DR. The wave mechanics of an atom with non-coulombic central field: parts I, II, III. *Proceedings of the Cambridge Philosophical Society* 1928;24:89; Fock V. Näherungsmethode zur Lösung des quanten-mechanischen Mehrkörperprobleme," *Zeitschrift für Physik*. 1930;61:126; Fock V. Näherungsmethoden zur Lösung des Quantenmechanischen Mehrkörperproblems, *Zeitschrift für Physik*. 1930;62:795.
- (47) Hohenberg P, Kohn W. Inhomogeneous Electron Gas. *Physical Review*. 1964;136(3B):B864-871.
- (48) Kohn W, Sham LJ. Self-Consistent Equations Including Exchange and Correlation Effects. *Physical Review*. 1965;140(4A):A1133.
- (49) Becke AD. Density-functional exchange-energy approximation with correct asymptotic behavior. *Physical Review A*. 1988;38(6):3098.
- (50) Perdew JP, Chevary JA, Vosko SH, Jackson KA, Pederson MR, Singh DJ, Fiolhais C. Atoms, molecules, solids, and surfaces: Applications of the generalized gradient approximation for exchange and correlation. *Physical Review B*. 1992;46(11):6671.

- (51) Scuseria GE. Ab initio calculations of fullerenes. *Science*. 1996;271(5251):942-945.
- (52) Frisch MJ, Headgordon M, Pople JA. A Direct Mp2 Gradient-Method. *Chemical Physics Letters*. 1990;166(3):275-280.
- (53) Chengteh L, Weitao Y, Parr RG. Development of the Colle-Salvetti correlation-energy formula into a functional of the electron density. *Physical Review B (Condensed Matter)*. 1988;37(2):785-789.
- (54) Yun Hang H, Ruckenstein E. Endohedral chemistry of C-60-based fullerene cages. *Journal of the American Chemical Society*. 2005;127(32):11277-11282.
- (55) Yun Hang H, Ruckenstein E. Quantum chemical density-functional theory calculations of the structures of defect C-60 with four vacancies. *Journal of Chemical Physics*. 2004;120(17):7971-7975.
- (56) Yun Hang H, Ruckenstein E. Ab initio quantum chemical calculations for fullerene cages with large holes. *Journal of Chemical Physics*. 2003;119(19):10073-10080.
- (57) El-Barbary AA, Lebda HI, Kamel MA. The high conductivity of defect fullerene C40 cage. *Computational Materials Science*. 2009;46(1):128-132.
- (58) Lu ZH, Lo CC, Huang CJ, Yuan YY, Dharma-wardana MWC, Zgierski MZ. Quasimetallic behavior of carrier-polarized C<sub>60</sub> molecular layers: Experiment and theory. *Physical Review B*. 2005;72(15):155440.
- (59) Frisch MJ, Gaussian 03, Revision D.01, Gaussian Inc., Wallingford CT. 2004
- (60) Ouahab L, Yagubskii E. Organic conductors, superconductors and magnets: from synthesis to molecular electronics. Kluwer Academic Publishers Netherlands. 2004;81-98.
- (61) Shemella P, Zhang Y, and Mailman M. Energy gaps in zero-dimensional graphene nanoribbons. *Applied Physics Letters*. 2007;91:042101.
- (62) Nakada K, Fujita M. Edge state in graphene ribbons: Nanometer size effect and edge shape dependence. *Physical Review B*. 1996;54:17954.
- (63) Cervantes-Sodi F, Csányi G, Piscanec S, and Ferrari AC. Edge-functionalized and substitutionally doped graphene nanoribbons: Electronic and spin properties. *Phys. Rev. B*. 2008;77:165427.

- (64) Huang B. Electronic properties of boron and nitrogen doped graphene nanoribbons and its application for graphene electronics. *Physics Letters A*. 2011; 375:845-848.
- (65) Yan QM, Huang B, Yu J, Zheng FW, Zang J, Wu J, Gu BL, Feng L, and Duan WH. Intrinsic current–voltage characteristics of graphene nanoribbon transistors and effect of edge doping. *Nano Letter*. 2007;7:1469-1473.
- (66) Peigney A. Specific surface area of carbon nanotubes and bundles of carbon nanotubes. *Carbon* 39. 2001;4:507-514.
- (67) Du X, Skachko I, Barker A, and Andrei EY. Approaching ballistic transport in suspended graphene. *Nature Nanotechnology*. 2008;3:491-495.
- (68) Dragoman M, Dragoman D. Graphene-based quantum electronics. *Progress in Quantum Electronics*. 2009;33(6):165-214.
- (69) Balandin AA, Ghosh S, Bao W, Calizo I, Teweldebrhan D, Miao F, Lau CN. Extremely High Thermal Conductivity of Graphene: Experimental Study. *Nano Letters*. 2008;8(3):902-907.
- (70) Lee C, Wei X, Kysar JW, Hone J. Measurement of the Elastic Properties and Intrinsic Strength of Monolayer Graphene. *Science*. 2008;321(5887):385-388.
- (71) Nair RR, Blake P, Grigorenko AN, Novoselov KS, Booth TJ, Stauber T, Peres NMR, Geim AK. Fine Structure Constant Defines Visual Transparency of Graphene. *Science*. 2008;320(5881):1308.